Yi *et al.*
Protection and Control of Modern Power Systems (2023) 8:27
https://doi.org/10.1186/s41601-023-00300-2

Protection and Control of
Modern Power Systems

REVIEW **Open Access**

Sensing as the key to the safety and sustainability of new energy storage devices

Zhenxiao Yi[1], Zhaoliang Chen[2], Kai Yin[3], Licheng Wang[4] and Kai Wang[1*]

Abstract

New energy storage devices such as batteries and supercapacitors are widely used in various fields because of their irreplaceable excellent characteristics. Because there are relatively few monitoring parameters and limited understanding of their operation, they present problems in accurately predicting their state and controlling operation, such as state of charge, state of health, and early failure indicators. Poor monitoring can seriously affect the performance of energy storage devices. Therefore, to maximize the efficiency of new energy storage devices without damaging the equipment, it is important to make full use of sensing systems to accurately monitor important parameters such as voltage, current, temperature, and strain. These are highly related to their states. Hence, this paper reviews the sensing methods and divides them into two categories: embedded and non-embedded sensors. A variety of measurement methods used to measure the above parameters of various new energy storage devices such as batteries and supercapacitors are systematically summarized. The methods with different innovative points are listed, their advantages and disadvantages are summarized, and the application of optical fiber sensors is emphasized. Finally, the challenges and prospects for these studies are described. The intent is to encourage researchers in relevant fields to study the early warning of safety accidents from the root causes.

Keywords New energy storage devices, Battery, Supercapacitor, Embedded sensors, Non-embedded sensors, Sensing

1 Introduction

The global energy crisis and climate change, have focused attention on renewable energy. New types of energy storage device, e.g., batteries and supercapacitors, have developed rapidly because of their irreplaceable advantages [1–3]. As sustainable energy storage technologies, they have the advantages of high energy density, high output voltage, large allowable operating temperature range, long cycle life, no obvious self-discharge phenomenon, and offer less pollution [4, 5]. They also have good performance in electrochemical storage and conversion technology [6, 7]. Therefore they are widely used in many fields, e.g., in portable electronic equipment, electric vehicles (EV) and hybrid electric vehicles (HEV), transportation industry, aerospace, military industry, and biomedical equipment, as shown in Fig. 1.

With the continuous reduction of the cost of the storage technologies and the continuous improvement of energy storage performance, storage capacities are significantly increased. This makes the quality, reliability and life (QRL) of new energy storage devices more important

*Correspondence:
Kai Wang
wangkai@qdu.edu.cn; wkwj888@163.com
[1] School of Electrical Engineering, Weihai Innovation Research Institute, Qingdao University, Qingdao 266000, China
[2] Qingdao No. 2 Middle School, Qingdao 266199, China
[3] Hunan Key Laboratory of Nanophotonics and Devices, School of Physics and Electronics, Central South University, Changsha 410083, China
[4] School of Information Engineering, Zhejiang University of Technology, Hangzhou 310014, China

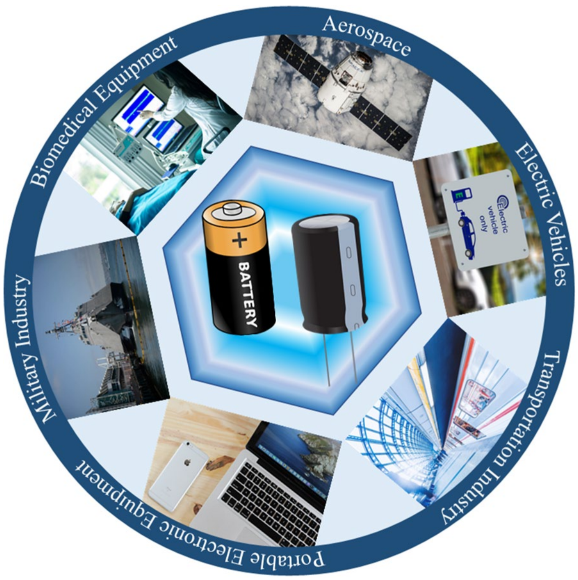

Fig. 1 Various application fields of new energy storage devices

than ever [8–10]. Therefore, an effective sensing system is crucial in their application.

Existing research relies on very limited measurements such as current, terminal voltage, and surface temperature [11], and most research focuses on methods based on electrochemical and physical models, and are data-driven [12, 13]. However, excessive reliance on imperfect data to establish a safety margin for batteries can eventually lead their underutilization. Because of the lack of sufficient detection parameters and limited understanding of the battery operation mechanism, there are challenges in accurately predicting the state and controlling the operational technology' the problems these cause can seriously affect the reliability and life of batteries [14–16]. In terms of ensuring the reliable operation, timely maintenance and echelon utilization, an effective sensing system with high performance and easy implementation can help to solve these problems.

Sensors having good performance in the measurements of voltage, current, temperature, strain, etc., are of great significance [17–20]. In existing practical applications, sensors are mainly divided into embedded and non-embedded sensors. These have their respective advantages and disadvantages in both the operational difficulty and accuracy of measurement parameters. They play irreplaceable roles on different occasions, and therefore this paper focuses on these two types.

The rest of this paper is organized as follows. Section 2 introduces the types of non-embedded sensors and their working principles. At the same time, the performance of new energy storage devices is introduced, and the characteristics of various types of sensors are summarized. Section 3 introduces the types of embedded sensors and their working principles, as well as their performance in new energy storage devices. It also compares them with non-embedded sensors, and puts forward some suggestions. Section 4 summarizes the characteristics of existing sensors used in new energy storage devices, and predicts future research and an improvement direction from the perspective of actual working conditions.

2 Application of non-embedded sensors in new energy storage devices

Non-embedded sensors mainly include current, voltage, temperature, and strain sensors, as well as several types combined with optical sensors. As their names suggest these can realize real-time detection of key parameters such as current, voltage, temperature, and stress in the working process, and do this without affecting the operation the storage devices [21, 22]. Therefore, by further analyzing the detected parameter data, it is possible to judge the working state of the device, such as SOC, SOH, and the remaining useful life (RUL) [23–26]. It can also provide an important reference for maintenance and other related work.

2.1 Current sensor

Non-embedded current sensors are mainly divided into Hall effect current and shunt resistance sensors [27]. The Hall effect sensor is a widely used and relatively simple method. Its working schematic diagram is shown in Fig. 2. By placing it in the magnetic field generated by the cable carrying the current, a voltage signal which is proportional to the current can be produced [28]. Since there is no direct electrical connection between the circuit of the Hall effect current sensor and that of the

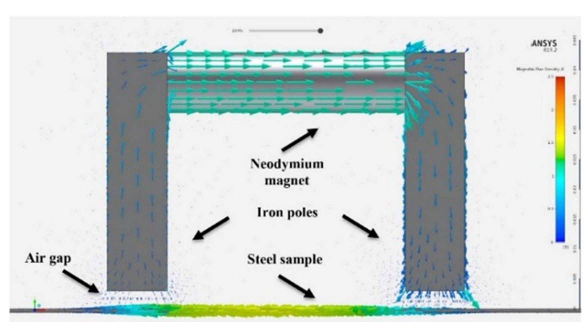

Fig. 2 Schematic diagram of working principle of Hall effect current sensor (Reproduced with permission from [28]. Copyright 2020, Journal of Magnetism and Magnetic Materials.)

energy storage device, it has the advantage of not requiring any other isolation measure.

However, because of its working mechanism, the external magnetic field will have an impact on the accuracy of the Hall effect sensor. In particular, when applied to the measurement of small current, there will be significant measurement errors [29], and the more complex the electromagnetic environment, the greater the impact on accuracy. In addition, Hall effect current sensors are expensive, large in size, and thus not suitable for sites with limited space. Currently, they are mostly used to measure the current of an entire battery pack.

Shunt resistors have the characteristics of high precision and low resistance, and are connected in series in the circuit under test [30]. The location of the shunt resistor in the current measurement circuit is shown in Fig. 3.

From Ohm's law, the current of the battery can be directly determined by using the ratio relationship between voltage and resistance. Compared with Hall effect current sensors, shunt resistors have simple structure, lower cost, wider range of applicable power levels, and current measurement accuracy of up to 0.1% or even higher.

However, since the shunt resistor is directly connected to the battery, it is necessary to provide additional isolation circuits in high-voltage scenarios, and this increases the complexity and cost of the system. In addition, since the shunt resistor is directly connected in series with the circuit, energy in the energy storage device will be consumed, which reduces the efficiency of the system [31, 32]. In addition, shunt resistance is also affected by ambient temperature, which limits its application.

To ensure the accuracy of the collected data, both Hall effect and shunt resistance sensors need amplifiers. Table 1 summarizes the advantages and disadvantages of both types of sensors.

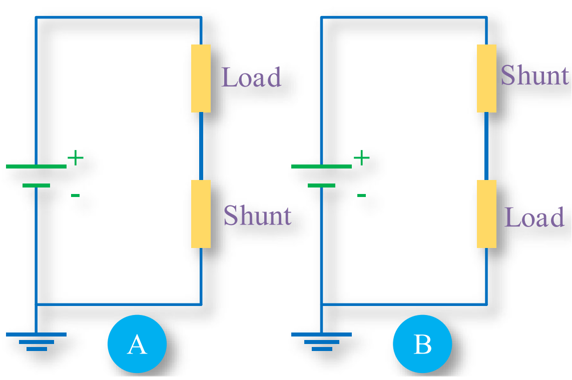

Fig. 3 Location of shunt resistors in current measurement circuits

2.2 Voltage sensor

At present, the most widely used voltage measurement method is to collect the voltage signal of a single battery using an integrated circuit and then convert it by an analog-to-digital converter (ADC) for further processing in the controller. Considering the limitation of space layout and cost, there are relatively few cases of developing special voltage sensors for battery cells and battery packs [33, 34]. Recently, some studies have realized the industrialization of battery voltage sampling chips, which can be applied to batteries. For example, NXP semiconductors (NXP) launched an intelligent battery monitoring chip mm9z1_638, which can accurately measure the voltage of the battery and simplify the application program, as shown in Fig. 4. At the same time, it can measure the current and temperature of the battery using a shunt resistor [35]. Because the integrated circuit voltage acquisition chip can meet the requirements of circuit board space layout and low power consumption, it is a promising voltage acquisition method.

2.3 Temperature sensor

The current temperature measurement methods mainly include thermocouples, thermistors, optical fiber sensing, and infrared imaging. By using the battery thermal model, related data processing and threshold judgment are realized in the battery management system (BMS) [36–38], while corresponding measures can be taken in time when thermal abnormalities occur. In addition, the

Table 1 Comparison of the advantages and disadvantages between Hall effect current sensor and shunt resistance

	Hall effect current sensor	Shunt resistor
Accuracy	Average accuracy	High accuracy
Influence	Independent of temperature; large deviation at low current	Easily affected by high temperature; Not suitable for high current as severe heating
Range	Large current range (Up to1000A)	Usually less than 20A
Volume	Large	Small size, easy to integrate
Energy dissipation	High	Low
Galvanic isolation	Demand	Not Required

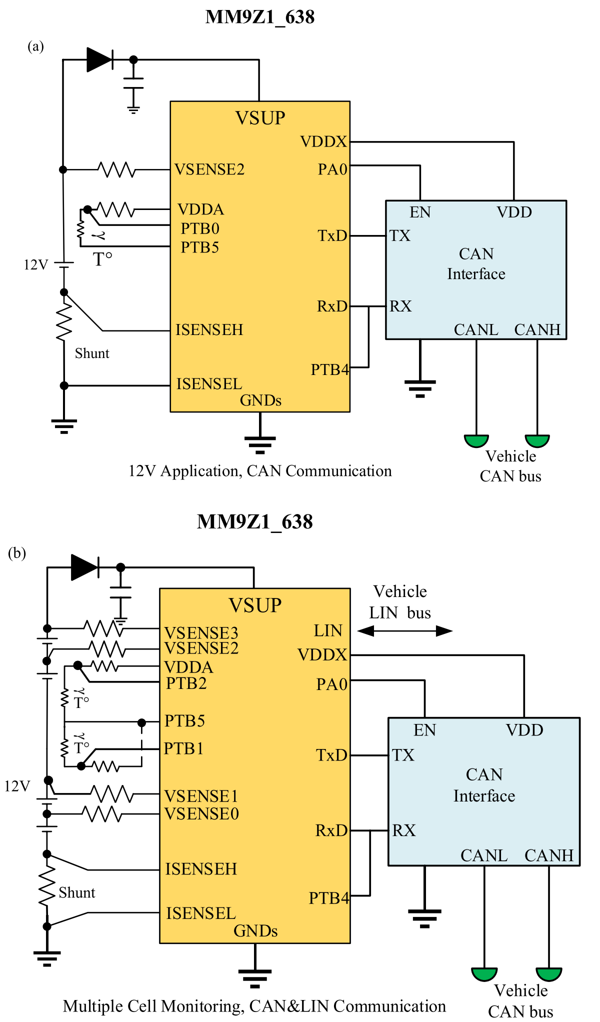

Fig. 4 Block diagram of voltage sensor simplified application

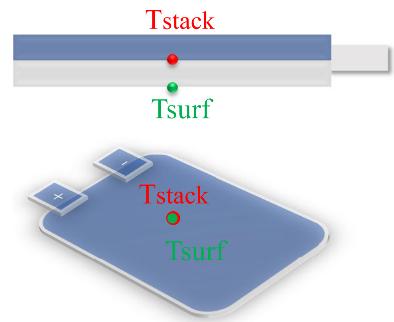

Fig. 5 Schematic diagram of thermistor installation (Reproduced with permission from [41]. Copyright 2015, Journal of the Electrochemical Society.)

thermal model can also be used to predict the battery SOC and SOH. This is of great significance for the timely maintenance and continuous use of the battery.

For the detection of the external temperature of the battery, reference [39] successfully used thermocouples to monitor the temperature of 16 different temperature points on the surface of large-size square soft-packed lithium-ion batteries. In 2017, reference [40] compared the fiber Bragg grating (FBG) and the K-type thermocouple sensors to monitor the temperature of the outer surface of the battery. The results showed that the FBG sensor had better resolution and 28.2% faster detection time than the thermocouple sensor. Thermistors are widely used because of their low cost, wide measurement range, and high-temperature sensitivity. In [41], thermistors were used to monitor the surface temperature of different types of batteries to study the related thermal behavior. It was found that the maximum temperature of the battery was linearly related to the discharge current, as shown in Fig. 5. At the same time, the influence of different environmental conditions on heat transfer was also discussed, and it was found that the temperature gradients in the bag-shaped and cylindrical batteries were generally different.

A resistance temperature detector (RTD) was also actively used for Lithium-Ion Battery (LIB) surface temperature measurement [42–44]. However, because the sensor size is incompatible with the battery design, it is not applied to the battery in an embedded manner, because it may damage the instantaneous performance and long-term cycle life of the battery.

The FBG sensor was used to measure the external temperature and strain of the battery. The sensitivity of the temperature sensor was 12 PM/℃, while the strain sensor had a unique sensitization structure, and the strain sensitivity reached 11.55 PM/℃ [45].

In [46], FBG sensors were respectively connected to the cathode and anode of a button battery and the cathode and outer surface of a cylindrical battery to detect the temperatures of the battery in real time. This can accurately and quickly detect battery temperature in the case of overcharge and short circuit. Its installation schematic diagram is shown in Fig. 6a,b. Since these methods are single point measurement techniques, they are insufficient for obtaining a spatially uneven temperature distribution.

In [47], three FBG sensors were installed on the diagonal of the bag battery, as shown in Fig. 6c. The experimental results showed that the FBG sensor has a faster response speed and higher sensitivity, and can solve the problem of not obtaining spatially uneven temperature distribution in single point measurement.

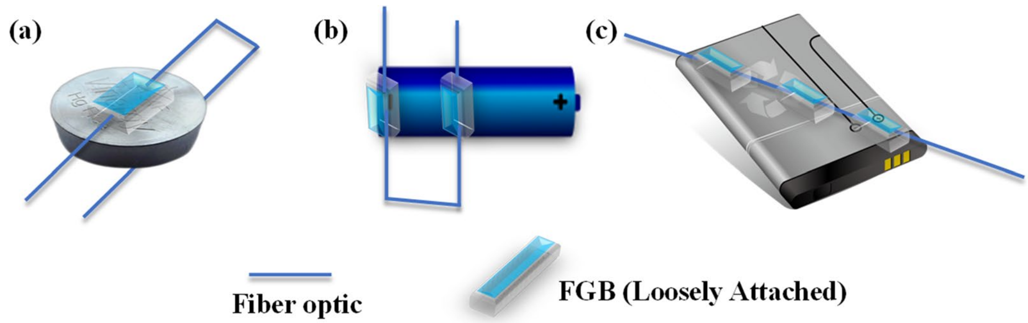

Fig. 6 Schematic diagram of different installation methods of FBG. **a** Button battery; **b** Cylindrical battery; **c** Pocket battery (Reproduced with permission from [46, 47]. Copyright 2014, IEEE Sensors Journal.)

Reference [48] analyzed the thermal behavior of a smartphone lithium-ion battery by considering environmental conditions (temperature and relative humidity). A network based on FBG sensors monitors the temperature at five different points on the surface of the lithium-ion battery. Figure 7 shows the schematic diagram of the experimental setup. This study quantified and elucidated the temperature values reached when the battery was exposed to three different environmental conditions. Through thermal mapping, it showed the areas of the LIB that needed to be cooled faster to improve its performance and thus avoid thermal runaway.

The application comparison of various non-embedded temperature sensors is shown in Table 2. As can be seen, the non-embedded temperature sensors can effectively measure the temperature outside the battery. The FBG sensor has the highest accuracy and sensitivity, with fast response. In addition, the distributed measurement method is more effective than the single-part measurement. However, because of the difference in temperature inside and outside the battery, the above methods have certain limitations.

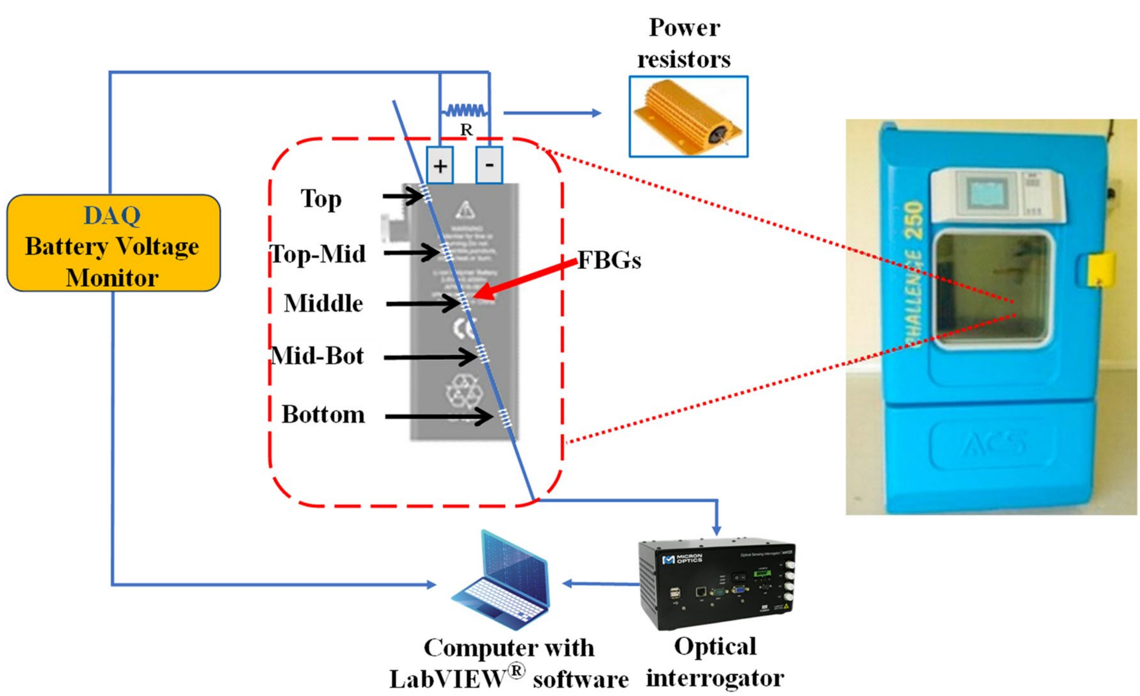

Fig. 7 Schematic of experimental set-up (left) and thermal chamber (right) (Reproduced with permission from [48]. Copyright 2019, Applied Thermal Engineering.)

Table 2 Application comparison of various non-embedded temperature sensors

Temperature sensor	Reference	Advantage	Disadvantage
Thermocouple	[39] [40]	Accurate measurement. Wide measuring range Strong anti-interference ability	Cumbersome to use Costly Non-linear Not suitable for high volume use
Thermistor	[41]	Low cost Wide measurement range and high sensitivity to temperature	Poor linearity Small adjustable range
RTD	[42–44]	High accuracy Stability	Incompatible sensor size and battery design Slow response
FBG	[49] [46] [47] [48]	High sensitivity Accurate measurement Fast response time	Exposed optical fiber is fragile Needs to be packaged

2.4 Strain sensor

Strain is also a very important parameter for monitoring battery condition and can often be reflected in changes in cell dimensions or surface pressure. Reference [50] found that the thickness of a pouch cell changed by as much as 4% of the total cell thickness during charging, while a fully charged prismatic cell with a hard shell also resulted in a 1.5% increase in cell thickness [51]. The reversible strain change in the LIB is directly related to the SOC, which makes it possible to estimate the SOC of the LIB by mechanical measurement [52, 53]. A relatively common and simple method is to measure the strain by detecting the total volume change of the battery with a strain gauge [54]. In addition, a load cell can be used. This uses a constraint fixture and is composed of an amplification load cell, connected in series with the battery, to apply the initial load to monitor the mechanical stress at the stack level in real-time [55]. It should be noted that the above methods cannot be directly applied to the onboard battery because of difficulty in the spatial arrangement of the pressure measuring components.

To solve the above problems, the General Electric Company has proposed a battery strain sensor based on battery expansion measurement [38, 56]. The sensor uses a flat coil to generate a high-frequency magnetic field, which induces a corresponding eddy current in the conductive material on the battery surface. Since the eddy current is inversely proportional to the distance between the batteries, the change in the battery volume can be obtained by measuring the eddy current strength.

In [57], a carbon nanotube (CNT)-based strain sensor was used to detect the irregular expansion of the cell. As shown in Fig. 8a, the sensor was developed by spraying a CNT coating on a stretchable substrate attached to the surface of the cell. After excluding the effect of temperature on the CNT resistance, the CNT strain sensor was verified for detecting a 6 mm expansion of the battery pack at 90° C. In general, the CNT sensor shows good performance in identifying minor LIB expansion.

Given that the strain caused by the volume expansion of the battery is usually not obvious, it is necessary to improve the sensitivity of the measurement. To this end,

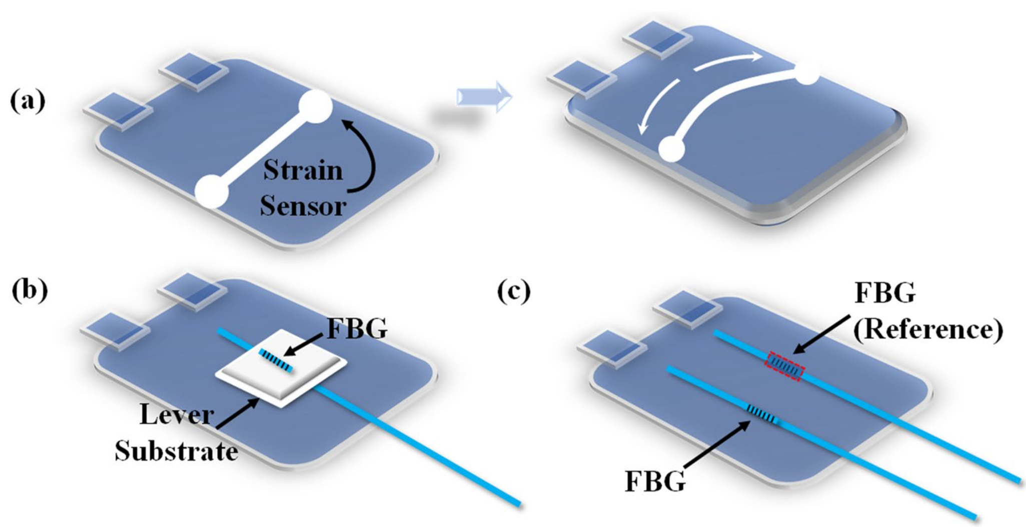

Fig. 8 Strain sensor: **a** Strain sensor based on CNT; **b** Optical FBG sensor with enhanced sensitivity; **c** Added strain compensated FBG sensor (Reproduced with permission from [58]. Copyright 2019, Actuators and Microsystems & Eurosensors.)

references [58, 59] designed an optical FBG sensor with enhanced sensitivity based on the strain concentration and lever amplification theory. An optical fiber is placed in the parallel bar mechanism in the base plate and fixed on the LIB surface, as shown in Fig. 8b. The mechanically amplified optical FBG sensor achieves higher strain sensitivity, thus improving the measurement accuracy.

In [60], the compensated strain was measured by arranging two FBG sensors in parallel on the LIB surface, as shown in Fig. 8c, with one rigidly bonded and the other loosely attached with thermal paste, while the remaining parameters remained consistent. It was found that the strain increase was more pronounced in the high SOC stage, while the subsequent stages effectively mitigated the strain accumulation by 15%. This provides important insight into the use of strain signals for real-time state estimation and optimal charging.

Since part of the strain is caused by temperature changes, a corresponding distinction needs to be made when temperature and strain change at the same time.

Reference [61] adopted an FBG sensor to simultaneously monitor the temperature and bidirectional strain of a prismatic Li-ion battery, as shown in Fig. 9. As can be seen, the measurements were performed by attaching two different types of FBG sensors to the Li-ion battery surface in the x-axis and y-axis directions. The strain-free FBG sensors (FBG1, FBG3, and FBG4) were only used to measure temperature changes and served as a reference, while the other FBG sensors (FBG2 and FBG5) were used to detect temperature and strain changes simultaneously. The study found that the deformation of the battery increases as temperature increase because of the thermal expansion of the battery material. This demonstrates the effectiveness of the reference FBG method, which can provide an alternative solution for real-time simultaneous sensing of temperature and strain. The application comparison of various strain sensors is shown in Table 3.

To sum up, non-embedded sensors have the advantages of relatively objective measurement accuracy and simple and non-destructive measurement. At the same time, there is no need to consider their influence on the internal structure of the energy storage device and the tolerance to the internal environment of the energy storage device. They have long-term stability and safety, and do not affect the performance of energy storage devices. The classification of non-embedded sensors and their practical applications are shown in Table 4.

However, the use of non-embedded sensors cannot fully perceive the internal "black box" in order to provide early warning of safety accidents from the root cause. In response to this problem, sensors are implanted inside the energy storage device, to detect the state of the energy storage device with high performance and in real-time.

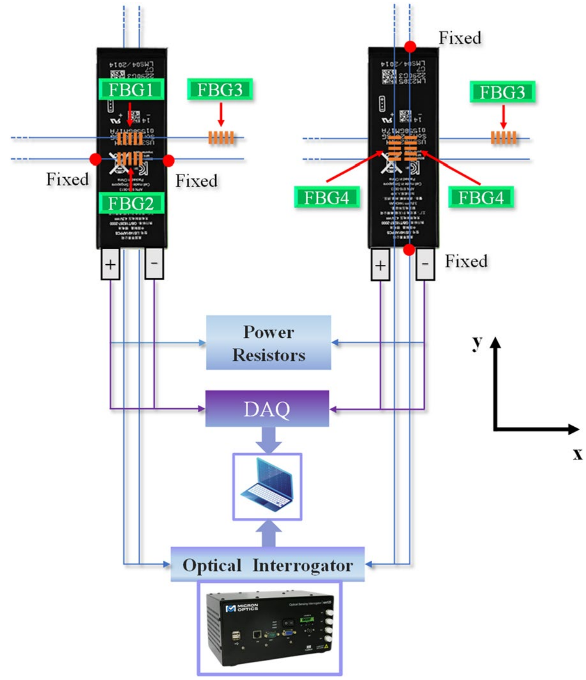

Fig. 9 Schematic diagram of the experimental setup for the reference FBG method (Reproduced with permission from [62]. Copyright 2018, Batteries-Basel.)

Table 3 Application comparison of various strain sensors

Strain sensor	Reference	Advantage	Disadvantage
Strain gauge	[51] [54]	Easy to apply and operate	Low accuracy
The weighing sensor	[55]	The method design is simple	Difficult spatial layout
Strain sensor based on magnetic field	[38, 56]	High measurement accuracy	Vulnerable to influence and interference
CNT	[57]	It can be decoupled from temperature measurement	Operation is difficult to implement
FBG	[58, 59] [61] [62]	High sensitivity and accuracy	Special treatment is required to ensure stability

3 Application of embedded sensors in new energy storage devices

Similar to non-embedded sensors, embedded sensors also include current, voltage, temperature and stress sensors, as well as several types of sensors combined with optical sensors [62]. Among the optical sensors, the FBG sensor can be expanded with a variety of optical sensors with different performance. These are mainly applied alone to measure the internal temperature, strain, and

Table 4 Classification of non-embedded sensors and their practical applications

Non-embedded Sensors	Reference	Classification	Practical limitations
Current sensor	[28] [30]	Hall-effect current sensor Shunt resistor	It is easily interfered with by external magnetic field and has large error when measuring small current, so is not suitable for measuring small current In practical applications, additional isolation circuits are required, and the cost is high while additional energy consumption will also occur
Voltage sensor	[33, 34] [35]	Smart battery monitoring chip	Integrated circuit is adopted with low power consumption and convenient layout, but it is difficult to design in practical application
Temperature Sensor	[39] [40] [41] [28–30] [46] [47] [48] [49] [63]	Thermocouple Thermistor RTD FBG	In practical applications, the cost is high, and it is troublesome to use and is not suitable for mass use The linearity in practical applications is poor, and it is not suitable for occasions requiring a large range of adjustment In practical application, there are problems such as slow response and difficult size design In practical application, because the optical fiber is relatively fragile, additional packaging measures are required
Strain sensor	[51] [54] [55] [38, 56] [57] [58, 59] [61] [62]	Strain gauge The weighing sensor Strain sensor based on magnetic field CNT FBG	Low accuracy in practical application Difficult spatial layout in practical application In practical application, the magnetic field can be easily disturbed which affects the measurement accuracy In practical application, it is difficult to operate, and the effect is poor when the strain is not obvious Additional cladding is required to ensure its good safety and stability in highly corrosive environments. At the same time, its long-term reliability is susceptible to bending and vibration

other parameters highly relevant to the SOC and SOH of the new energy storage devices, overcoming the limitations of external detection [64–66]. At the same time, there is no impact on the performance of the energy storage devices. Therefore, it is also important for the later maintenance of energy storage devices and other related work.

3.1 Current sensor

Considering the limitation of space layout and cost, there are relatively few developed special current sensors for new energy storage devices. Reference [67] developed a flexible three-in-one embedded battery micro-sensor in view of the shortcomings of non-embedded current sensors. This solution regards the equivalent series resistance of the battery as a shunt resistance, as shown in the Lithium-ion battery circuit model in Fig. 10. At the same time, it can withstand the harsh environment inside the battery. A current microsensor consists of a pair of voltage-measuring probes and a pair of resistance-measuring probes that calibrate the current according to Ohm's law. This tiny sensor can accurately measure the battery's internal current with negligible impact on the battery performance.

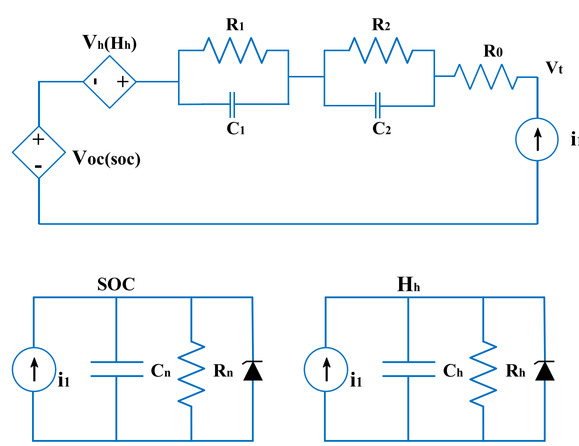

Fig. 10 Lithium-ion battery circuit model based on second-order RC design (Reproduced with permission from [68]. Copyright 2017, IEEE Transactions on Vehicular Technology.)

3.2 Voltage sensor

Since the embedded voltage sensor can measure some parameters that otherwise cannot be measured by non-embedded sensors, such as distributed current and overpotential, voltage measurement is also extended from the

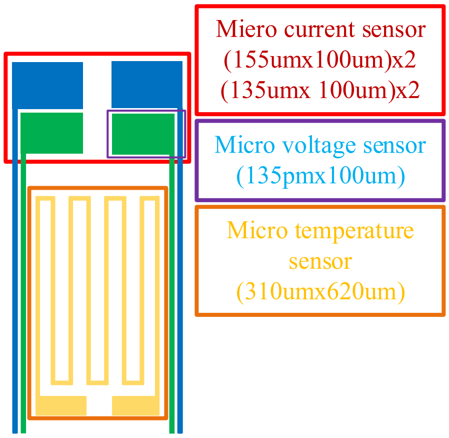

Fig. 11 Structure diagram of three-in-one micro-sensor (Reproduced with permission from [74]. Copyright 2015, Sensors.)

terminal to the inside of the battery. These rich parameters can help to estimate the SOC and SOH of new energy storage devices such as batteries and supercapacitors through electrochemical (EM), equivalent circuit (ECM), and artificial intelligence models (AIM) [68–72].

In [73], a flexible three-in-one micro-sensor was developed that can withstand the harsh internal environment of lithium batteries and give timely feedback of the internal information to the outside in advance for safe management without destroying the structure of the battery. This embedded voltage measurement method mainly adopts the idea of integrating a voltage sensor and a temperature/current sensor, and is embedded in the battery to realize the in-situ measurement of current, voltage, and internal temperature. The structure diagram is shown in Fig. 11. In addition, this embedded miniature sensor can also detect parameters such as distributed current and overpotential that cannot be measured by external sensors.

This internal property is more directly related to the multi-physical process of the battery, which can better detect the state of the battery and take corresponding measures in time. This unique advantage offers a future research direction.

3.3 Temperature sensor

Since the components of most new energy storage devices generally have a multi-layer structure, thermal conductivity is poor [58, 74]. Therefore, although the heat generated is modest, it is difficult for it to be dissipated to the outside. In addition, as large-scale energy storage devices have become a trend, it will cause the internal temperature of the energy storage device to be more non-uniform, and thus the in-situ measurement of the internal temperature of the energy storage device is very important. Embedded temperature sensors are mainly divided into thermocouples, thermal resistance sensors, and various optical fiber sensors.

A thermocouple has the advantages of low cost, small size, and high sensitivity. Reference [75] embedded a T-type thermocouple into a 18,650 cylindrical lithium battery to provide a temperature reference, and at the same time, the fault diagnosis method based on the thermal model was verified. In [76], a K-type thermocouple was embedded in the battery cell to measure the temperature. It proved that there was a significant difference between the internal and external temperatures of the battery, which also validated the importance of embedded sensors in the temperature measurement of energy storage devices. In [77], it was verified that the battery performance was not affected by the embedded thermocouple by fabricating a lithium-ion battery with an embedded thermocouple. However, it was unclear whether there would be potential impact on the long-term cycle life of the battery.

Thermal resistance sensors can be subdivided into thermistors and RTDs. However, because of the incompatibility of the size of the sensors and the design of the energy storage device, they are rarely used as embedded sensors so as to avoid affecting the performance and long-term cycle life. However, high-precision NTC thermistors can be used to fabricate thin-film sensors for in-situ distributed measurement of the internal temperature of Li-ion batteries [74]. This method is more sensitive than the non-embedded temperature sensors, and has the advantage of faster response. The experimental results show that this method has no great influence on the capacity, electrolyte, and electrode of the battery.

Reference [36] used a thin-film RTD sensor with seven detection points to realize a multi-point measurement of the internal temperature of lithium batteries. This distributed method has higher accuracy than the single-point measurement, while the effect on the performance of the battery is also negligible.

Fiber optic sensors also have a wide range of applications in measuring the temperature of energy storage devices. For example, reference [78] proposed a method to seal fiber Bragg gratings (FBGs) embedded in pouch cells by filling gaps with heat-sealing materials to monitor the internal stress and temperature of the cells to estimate the SOC. In [79], an optical fiber sensor embedded in the lithium battery was used to monitor the battery status. The optical fiber can withstand a temperature of $-200 \sim 800$ ℃ given a suitable coating. This is far beyond the normal working temperature of the battery. In addition, there is little effect on battery capacity and life after cycling. In [80], the FBG sensor was implanted inside the battery to monitor the

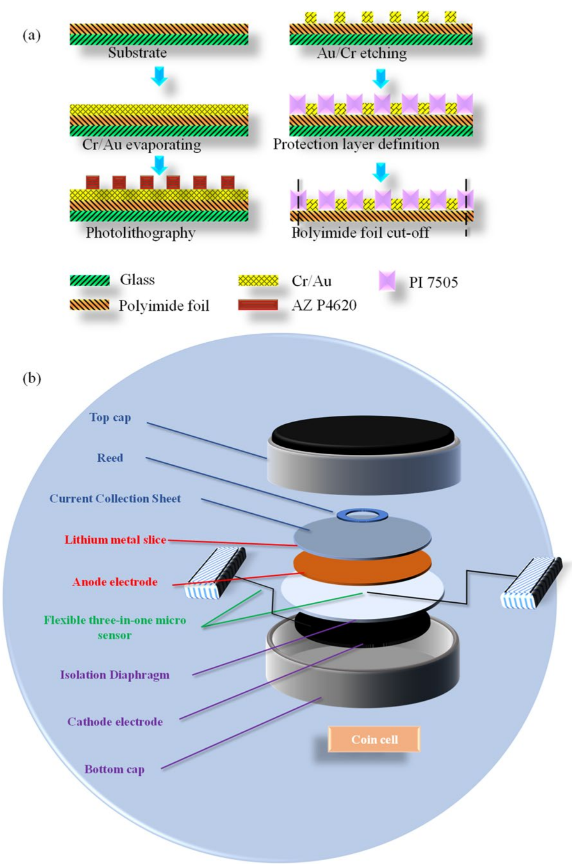

Fig. 12 Schematic diagram of the production process and packaging components. **a** Production process of flexible three-in-one microsensors; **b** Schematic diagram of the packaged components of the embedded flexible triple-micro sensor in the coin cell (Reproduced with permission from [82]. Copyright 2016, Sensors (Basel, Switzerland).)

temperature and compared with the external measurement. It was found that at a charging rate of 5C, the internal sensor detected a temperature change of 4 °C compared to a change of 1.5 °C detected by the external sensor, demonstrating that the internal temperature monitoring can better reflect the internal thermal behavior of the battery.

The results from further experimental studies, in which the FBG sensor was embedded in the core void of a 18,650 battery and a pre-drilled hole was used in the middle of the battery cover to measure the temperature inside the battery, showed that the core temperature in the battery is about 5 °C higher than the surface temperature of the battery. This further proves the difference between the internal and external temperatures of different types of batteries, demonstrating the importance of internal temperature detection [81, 82]. Reference [83] developed a flexible three-in-one microsensor by applying microelectromechanical systems (MEMS) technology to a flexible substrate. This micro-sensor can not only withstand the harsh environment inside the lithium battery but also measure the internal temperature, voltage, and current of the battery in real-time. The timely feedback of the internal information to the outside in advance for safety management can avoid damage to the structure of lithium batteries, can help future improvements in lithium battery design and material development. The production process and packaging components are shown in Figs. 12a, b, respectively.

Considering the limitations of current single-point detection and external detection of lithium-ion battery packs, reference [84] proposed and designed a distributed optical fiber in-situ monitoring method for the health state of the temperature field in lithium-ion batteries. The optical fiber FBG temperature sensor was embedded in the lithium battery, and the distributed real-time monitoring of the distribution state and evolution law of the temperature field in the lithium-ion battery under different operating environments were realized theoretically and experimentally. In addition, this method also has the advantages of distributed multi-point simultaneous monitoring and low cost. This can provide a reference for early warning and assessment of the health status of large-scale lithium-ion battery integrated components in the future.

The thermal coupling model of a single cell was established, as shown in (1), while the thermophysical parameters of each part of the 5500 mAh lithium-ion battery in the experiment are shown in Table 5.

Table 5 Thermal physical parameters of each part of the 5500 mAh lithium-ion battery

Material	Density/(kg m^{-3})	Thermal conductivity/(W m^{-1} K^{-1})	Specific Heat Capacity/ (J kg^{-1} K^{-1})
Single cell	2122	k_x:21; k_y:21; k_z:0.48	933
Positive tap	2719	202.4	871
Negative tap	8978	387.6	381
Separator	1008	0.3344	1978
Case	8193	14.7	439.3

In (1), ρ_P, ρ_n and ρ_r are the densities of the positive electrode current collector, the negative electrode current collector and the battery plate, respectively. C_P, C_n and C_r are the positive electrode current collector, the negative electrode current collector and the specific heat capacity of the battery plate, respectively. q_{fp}, q_{fn} and q_{fr} are the heat dissipation rates of the positive electrode sheet current collector, the negative electrode sheet current collector and the battery plate, respectively. The heat dissipation rates of the positive and negative electrode sheets are $\frac{q_{fp}}{dt} = \frac{q_{fn}}{dt} = 0$, while k_{px}, k_{py}, and k_{pz} are the thermal conductivities along the x, y, and z directions in the positive electrode sheet, respectively. ϕ_p and ϕ_n are the electrical conductivities of the positive and negative plates, respectively, and σ_{cp} and σ_{cn} are the currents flowing through the positive and negative plates, respectively. I_{tp} and I_{tn} are the respective positive and negative plates, h_p and h_n are the thickness of the sheet, while S_p and S_n are the areas in the x and y planes of the positive and negative sheets, respectively.

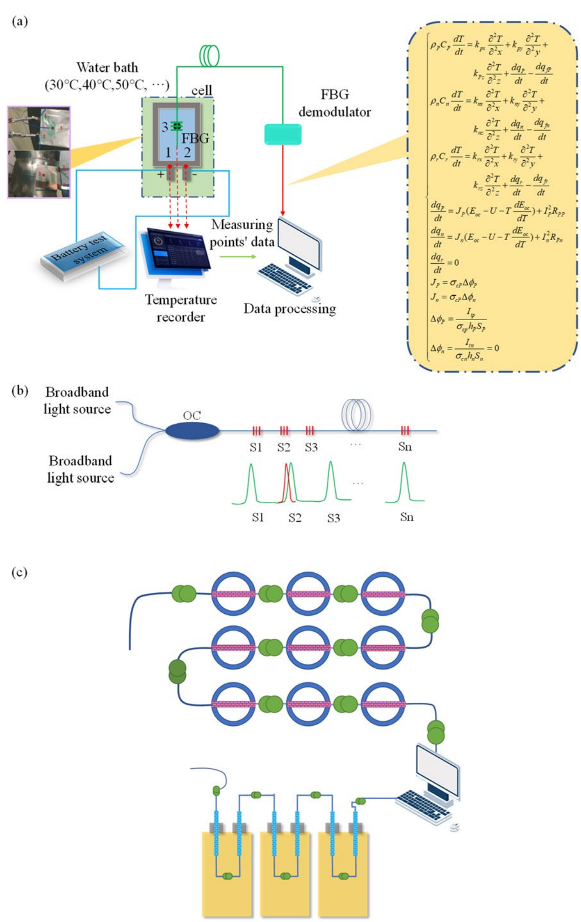

Fig. 13 Schematic diagram of each part of the experimental device. **a** Experimental device; **b** Fiber Bragg Grating Temperature Sensor Distributed Sensing System; **c** Embedding method of FBG (Reproduced with permission from [86]. Copyright 2020, Chinese Journal of Lasers.)

The schematic diagram of the experimental set-up is shown in Fig. 13a, while the fiber grating temperature sensor distributed sensing system is shown in Fig. 13b. Wavelength division multiplexing (WDM) technology is used to realize multiple gratings (each grating has different grating constants) in series on one fiber. An FBG embedding method was also proposed, as shown in Fig. 13c. Through the cascade of sensor arrays formed by the series connection of transmission fibers or the Organization of Fast Relief & Development (OFDM) technology, not only real-time continuous in-situ monitoring of temperature fields in multicell modules can be realized, but also an effective optical fiber sensor is embedded inside the lithium battery to monitor quantities such as temperature, vibration, strain, etc., without affecting the battery performance and the optical fiber sensing performance. At the same time, the method of selecting temperature characteristic points in combination with thermal simulation optimizes the placement position of the sensor and the usage of the sensor. This all reduces the difficulty of the process and the cost of the demodulation equipment [85]. This has a very important guiding significance for the development of smart new energy functions in the future. The application comparison of various embedded temperature sensors is shown in Table 6.

$$\begin{cases} \rho_P C_P \dfrac{dT}{dt} = k_{px}\dfrac{\partial^2 T}{\partial^2 x} + k_{py}\dfrac{\partial^2 T}{\partial^2 y} + \\ k_{Pz}\dfrac{\partial^2 T}{\partial^2 z} + \dfrac{dq_P}{dt} - \dfrac{dq_{fP}}{dt} \\ \rho_n C_n \dfrac{dT}{dt} = k_{nx}\dfrac{\partial^2 T}{\partial^2 x} + k_{ny}\dfrac{\partial^2 T}{\partial^2 y} + \\ k_{nz}\dfrac{\partial^2 T}{\partial^2 z} + \dfrac{dq_n}{dt} - \dfrac{dq_{fn}}{dt} \\ \rho_r C_r \dfrac{dT}{dt} = k_{rx}\dfrac{\partial^2 T}{\partial^2 x} + k_{ry}\dfrac{\partial^2 T}{\partial^2 y} + \\ k_{rz}\dfrac{\partial^2 T}{\partial^2 z} + \dfrac{dq_r}{dt} - \dfrac{dq_{fr}}{dt} \\ \dfrac{dq_P}{dt} = J_P(E_{oc} - U - T\dfrac{dE_{oc}}{dT}) + I_P^2 R_{PP} \\ \dfrac{dq_n}{dt} = J_n(E_{oc} - U - T\dfrac{dE_{oc}}{dT}) + I_n^2 R_{Pn} \\ \dfrac{dq_r}{dt} = 0 \\ J_P = \sigma_{cP}\Delta\phi_P \\ J_n = \sigma_{cP}\Delta\phi_n \\ \Delta\phi_P = \dfrac{I_{tp}}{\sigma_{cp} h_P S_P} \\ \Delta\phi_n = \dfrac{I_{tn}}{\sigma_{cn} h_n S_n} = 0 \end{cases} \tag{1}$$

Table 6 The application comparison of various embedded temperature sensors

Temperature Sensor	References	Advantage	Disadvantage
Thermocouple	[75] [76] [77]	Low cost Small size and high sensitivity	Low precision Poor stability
Thermal resistance			
Thermistor RTD	[74] [36]	High sensitivity Small size Fast response time Low cost	Wiring is technically difficult
FBG	[78] [79] [80] [83] [84]	Small size Anti electromagnetic interference Corrosion resistance It can be multiplexed	Exposed optical fiber is fragile and needs to be packaged

3.4 Strain sensor

For battery monitoring, strain is as important as temperature because of uneven electrode stress accumulation, which reduces the capacity and power of the battery [86, 87]. Electrode stress can usually be reflected by dimensional changes or surface pressure of the electrodes and/or the entire cell.

FBG sensors were implanted inside a battery to monitor strain and temperature and it was found that there was a stable strain behavior inside the battery and the temperature difference between the inside and outside of the battery was about 10 °C during charge and discharge cycles [88]. In [89], FBG sensors were implanted into the commercial 18,650 cells to monitor changes in temperature and pressure inside the cells, and it found that implanting FBG sensors did not affect the electrochemical performance of the cells after comparing the capacity retention of the cells with and without fiber optic sensor implantation for 100 cycles.

In [90], the functionality of the optical FBG sensor was enriched by adding optical FBG components, as shown in Fig. 14. Using the new method, the internal temperature, strain, and refractive index changes of the LIB can be detected simultaneously. It is foreseeable that emerging FBG designs will continue to be less invasive while maintaining measurement fidelity. This offers a promising research direction.

However, due to the inherent ability of optical FBG sensors to simultaneously measure temperature and strain, the two variables are inherently coupled together and a reasonable decoupling method needs to be designed.

In [91], the coupling effect of strain was excluded by inserting a loosely arranged single-mode fiber optic sensor with a diameter of 150 μm into the middle of the jelly roll of a 18,650 cell, as shown in Fig. 15. The SMF-FBG and micro-structured fibers were pre-bonded with

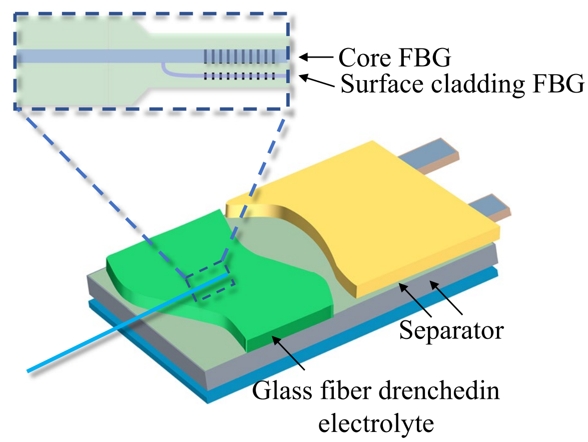

Fig. 14 FBG sensor with added optics (Reproduced with permission from [72]. Copyright 2019, Batteries-Basel.)

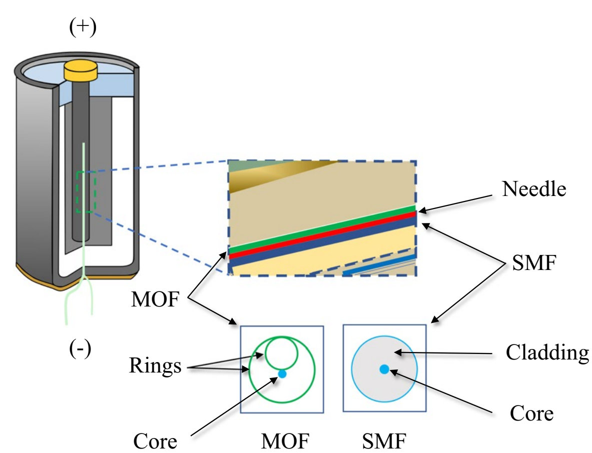

Fig. 15 Schematic diagram of the 18,650 battery embedded with a single-mode fiber optic sensor (Reproduced with permission from [73]. Copyright 2020, Nature Energy.)

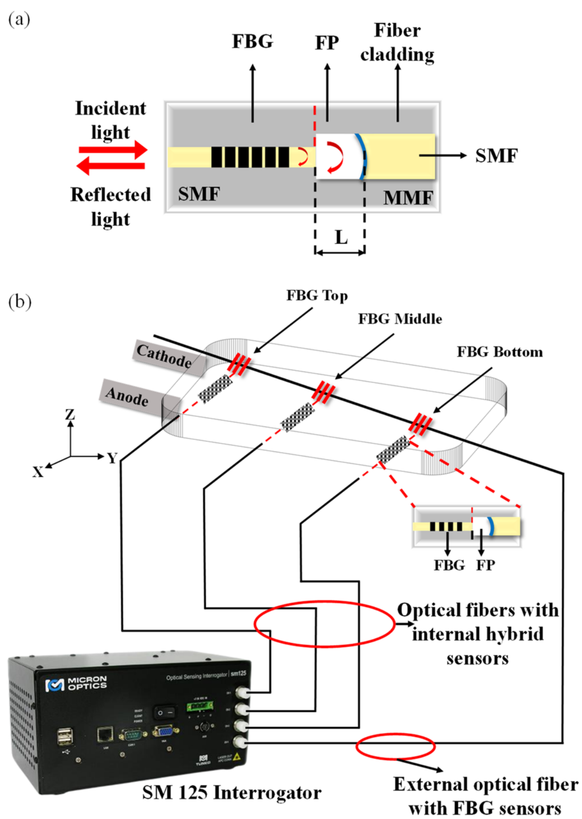

Fig. 16 Schematic of the hybrid sensor and experimental setup. **a** Hybrid sensor; **b** Experimental device (Reproduced with permission from [94]. Copyright 2019, Journal of Power Sources.)

parallel pins to ensure consistent sensing in position. The optical FBG sensor was then passed through the pre-drilled hole into the center void of the jelly roll. For insulation purposes, the interface between the cell and the needle was further sealed with epoxy. By using the above structure, simultaneous decoding of battery temperature and pressure can be achieved.

In [92], a hybrid sensing network was proposed to discriminate between strain and temperature inside a Li-ion battery, as shown in Fig. 16. The hybrid sensor consisted of an FBG sensor and an FPI sensor capable of measuring both temperature (δT) and strain (δε). It was also found that the strain variation was related to the temperature variation. The results showed that the higher strain variation was caused by the higher temperature variation. By comparing the experimental results obtained at three different positions, the effectiveness and feasibility of the discrimination method proposed in this study were proved.

The classification of embedded sensors and their practical applications are shown in Table 7.

Table 7 Classification of embedded sensors and their practical applications

Embedded Sensors	Reference	Classification	Practical limitations
Current sensor	[67]	Based on the second-order RC design	The current needs to be calibrated according to Ohm's law, and errors may occur in actual operation, which will affect the accuracy
Voltage sensor	[73]	Three in one micro sensor	It has no effect on the performance of the battery, but the design is complicated and the operation technology is difficult
Temperature Sensor	[36] [74] [75] [76] [77] [78] [79] [80] [83] [84]	Thermocouple NTC Thin film RTD FBG	In practical application, there may be potential impact on the long-term cycle life of the battery In practical applications, the size of the sensor and the design of the energy storage device are difficult to be compatible, which may affect the performance and long-term cycle life of the energy storage device In practical application, there are problems such as complex manufacturing process and difficult installation In practical applications, due to the relative fragility of optical fiber, other packaging measures such as corrosion resistance and ensuring the stability of optical fiber need to be considered
Strain sensor	[85] [88] [89] [90] [91] [92]	FBG FBG sensor with added optics SMF-FBG (FBG-FPI	In practical applications, since the two variables, temperature and strain, are intrinsically coupled together, a reasonable decoupling method needs to be designed In practical applications, the two variables of temperature and strain can be decoupled, but this will also lead to difficult design problems

3.5 Fiber optic sensor

Through the above comparative analysis, it can be seen that the fiber optic sensor FBG has the advantages of lightness, electrical insulation, anti-static discharge, anti-electromagnetic interference, and high-sensitivity distributed testing of multi-parameters (such as temperature and strain) in both non-embedded and embedded sensors [93–95]. The advantages of this will ensure that this will be a development trend. For the sake of completeness, fiber optic sensors are further described below.

In addition to sensitively measuring the temperature and strain of novel energy storage devices, fiber optic sensors can also measure parameters that are directly related to the SOC and SOH, enabling their estimation [96]. Among them, optical FBG sensors have been widely studied and used to measure parameters such as local static and fluctuating temperature, strain, and refractive index (RI) in electrochemical systems that are highly correlated to the state of energy storage devices. An FBG sensor consists of a short length of single-mode fiber with a photo-induced periodic modulation of RI in the core, typically a few millimeters in length. When the FBG sensor is illuminated with a broadband optical signal, as shown in Fig. 17a, the wavelength of the reflected signal can be given as:

$$\lambda_{\mathrm{B}} = 2n_{eff}\Lambda \tag{2}$$

where Λ is the grating period, n_{eff} is the effective RI of the fiber core, and λ_{B} is the so-called Bragg wavelength.

When the FBG sensor is externally affected, taking temperature T (Fig. 17b) and strain ε (Fig. 17c) as examples, the responses to temperature change ΔT and strain change $\Delta\varepsilon$ can be determined by:

$$\Delta\lambda_B = \lambda_B\left(\frac{1}{n_{eff}}\frac{\partial n_{eff}}{\partial T} + \frac{1}{\Lambda}\frac{\partial \Lambda}{\partial T}\right)\Delta T = \lambda_{\mathrm{B}}(\alpha+\xi)\Delta T = K_T\Delta T \tag{3}$$

$$\Delta\lambda_B = \lambda_B\left(\frac{1}{n_{eff}}\frac{\partial n_{eff}}{\partial \varepsilon} + \frac{1}{\Lambda}\frac{\partial \Lambda}{\partial \varepsilon}\right)\Delta \varepsilon = \lambda_{\mathrm{B}}(1-p_e)\Delta \varepsilon = K_\varepsilon\Delta \varepsilon \tag{4}$$

where λ_{B} is the shift in the Bragg wavelength, α and ξ are the thermal expansion and thermo-optic coefficients

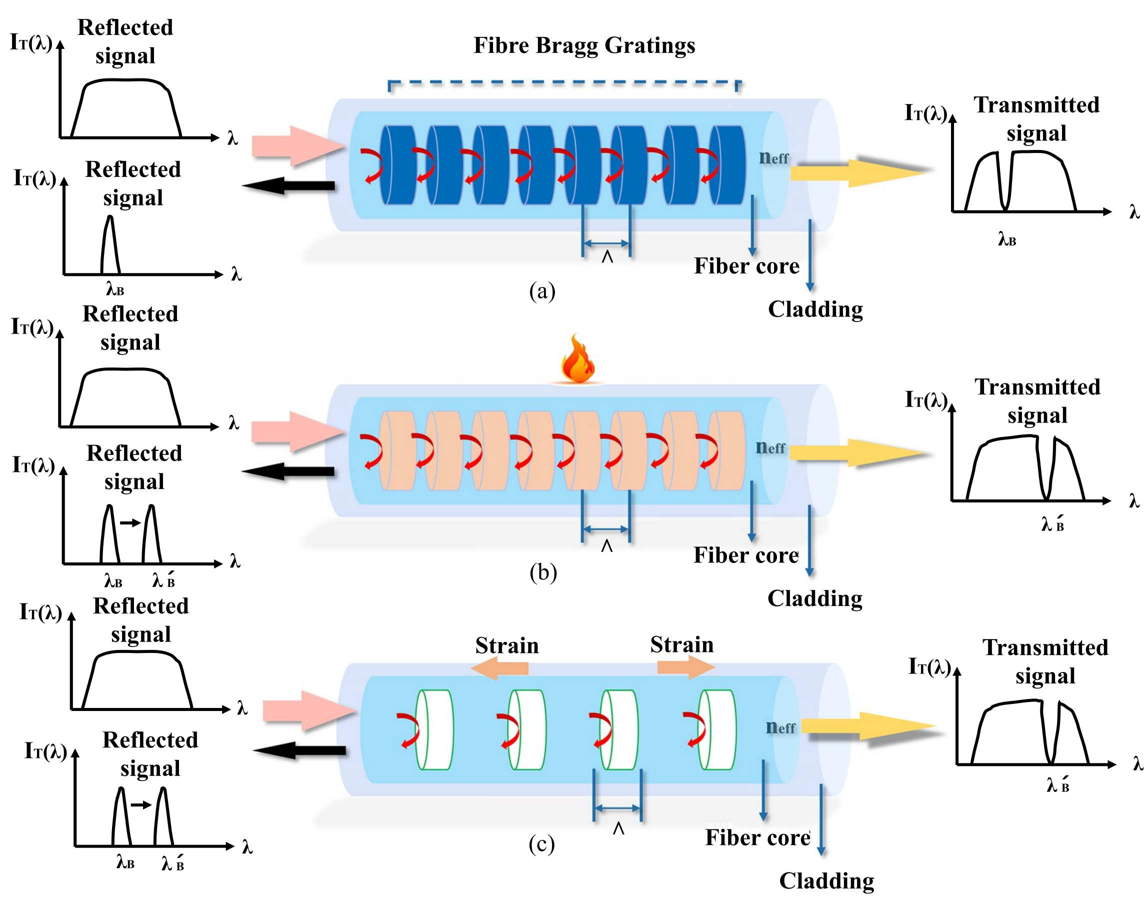

Fig. 17 Operating principle of optical fiber sensor. **a** Only the light signal illuminates the FBG sensor; **b** Affected by temperature; **c** Affected by strain (Reproduced with permission from [96]. Copyright 2022, Energy & Fuels.)

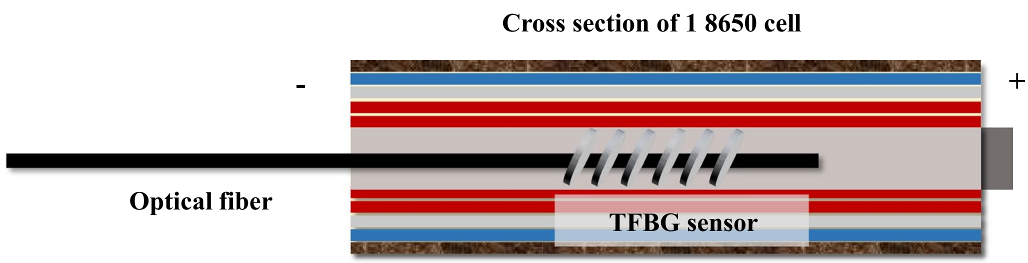

Fig. 18 Schematic diagram of a typical TFBG sensor (Reproduced with permission from [99]. Copyright 2018, Light: Science & Applications.)

of the optical fiber material, respectively. P_e is the photoelastic constant of the fiber, while K_T and K_e are the temperature and strain sensitivities, respectively.

On the basis of the FBG sensor, the tilted fiber Bragg grating (TFBG) sensor has a special configuration, which can enhance the sensitivity of the surrounding refractive index (SRI). In [97], a TFBG sensor was adopted to detect SOC for supercapacitors. In a typical TFBG sensor, as shown in Fig. 18, the tilt angle θ induces efficient coupling of partially transmissive core modes with either co-propagating or counter-propagating cladding modes, depending on θ.

Reference [98] investigated the reflectivity of commercial graphite anodes and conducted fiber-optic evanescent wave spectroscopy of electrochemically lithiated graphite in Swagelok lithium-ion batteries and found similar SOC-dependent trends. This indicates that the SOC of Li-ion batteries can be measured by embedded fiber-optic sensors. Reference [37] integrated fiber-optic sensors with cylindrical and pouch-shaped lithium batteries, and demonstrated a fiber-optic evanescent wave sensor integrated with a graphite anode to solve the problems of electrode lifetime attenuation and deformation. Being able to do this is important in monitoring the SOC and SOH of Li-ion batteries.

The change of SRI can be measured by detecting the change of the grating transmission spectrum of the TFBG, which can effectively detect the SOC of the supercapacitor. Reference [97] demonstrated for the first time a surface plasmon resonance (SPR)-based fiber-optic sensor for monitoring electrochemical activity in supercapacitors. From this, a new fiber optic sensor named

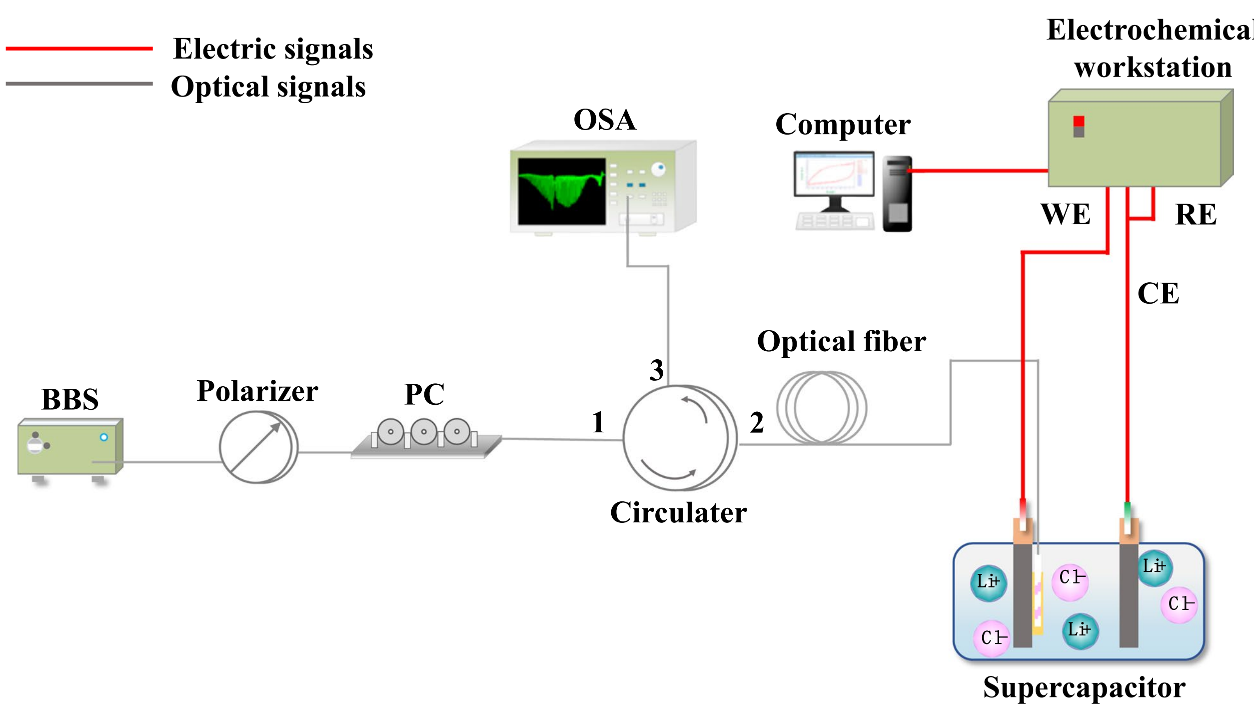

Fig. 19 Schematic diagram of the experimental setup of the TFBG-based SPR fiber optic sensor (Reproduced with permission from [99]. Copyright 2018, Light: Science & Applications.)

TFBG-based SPR was proposed for in-situ monitoring of supercapacitor SOC. The proposed plasmonic TFBG sensor was attached to one electrode of the supercapacitor to monitor the electrochemical activity. Figure 19 shows the experimental setup. The study measured the charge density and the SOC, and the results showed that the spectral response of the SPR mode of TFBG was directly related to the charge density and SOC of the supercapacitor. Therefore, by detecting changes in the position and intensity of the reflection spectrum, changes in charge density and SOC during charge and discharge can be monitored.

In [99], a method based on localized surface plasmon resonance (LSPR) was first proposed for SOC monitoring of supercapacitors. Gold nanoparticles were deposited on the core of a multimode fiber to create an LSPR sensing area (10 mm), and a silver mirror was coated on the end of the fiber (2 mm), as shown in Fig. 20a. The SOC was monitored using a three-electrode supercapacitor, as shown in Fig. 20b. Ag/Ag/Cl was used as the reference electrode (RE), Pt was used as the counter electrode (CE) and MnO_2 based on carbon fiber fabric was used as the working electrode (WE), while the LSPR fiber optic sensor was hooked near the electrodes. The LSPR sensor was used for real-time online SOC monitoring of electrodes in supercapacitors during charging and discharging, and it found that the intensity shift of the LSPR spectrum had a good linear relationship with the SOC of the electrode.

The various optical sensors based on fiber optic sensors have excellent performance in both measuring highly state-dependent parameters such as temperature and strain of various batteries and supercapacitors, and directly characterizing the SOC and SOH. A summary of various fiber optic sensing methods is shown in Table 8.

3.6 Challenges and outlook

Safety and stability are the keys to the large-scale application of new energy storage devices such as batteries and supercapacitors. Accurate and robust evaluation can improve the efficiency of power storage cell operation [130, 131]. Therefore, a method to obtain high-precision parameters that are highly correlated with their states is

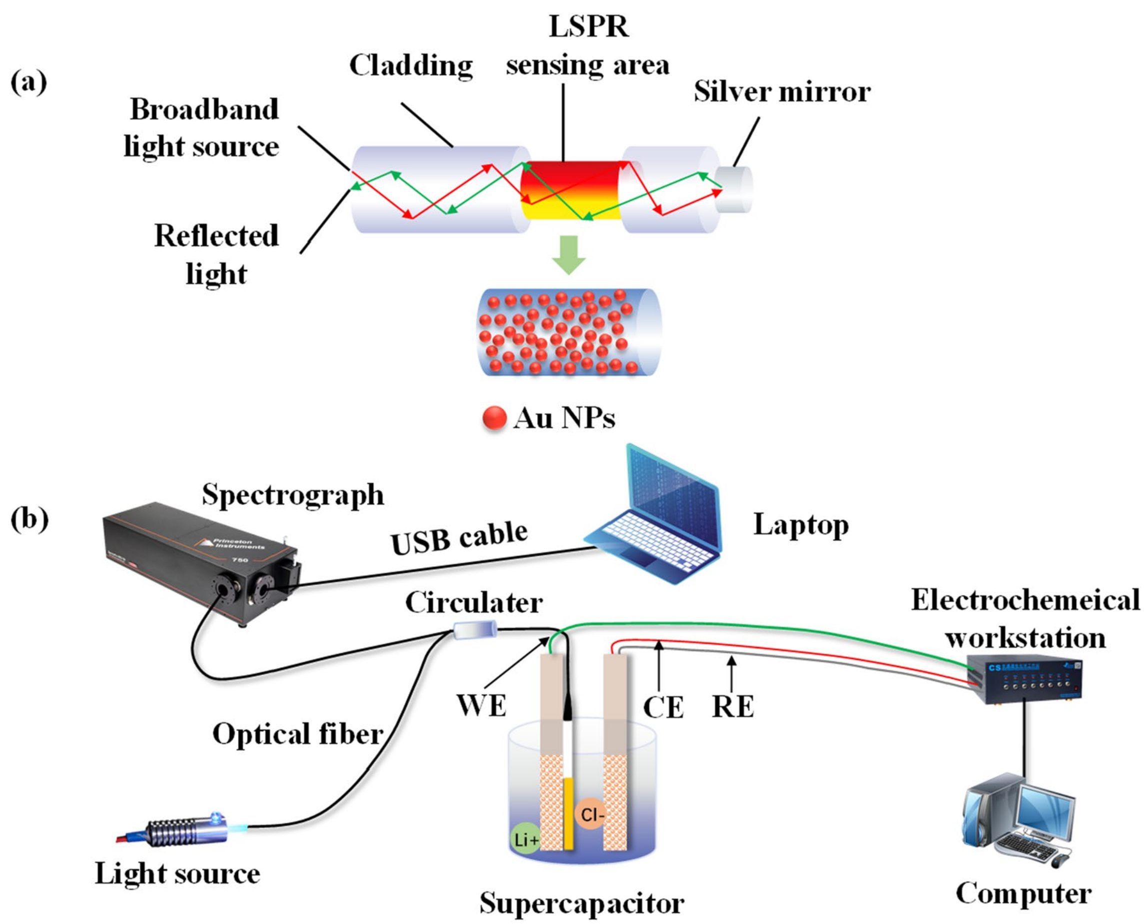

Fig. 20 LSPR optical fiber sensor. **a** Schematic structure; **b** Experimental setup for SOC monitoring (Reproduced with permission from [102]. Copyright 2020, Nanophotonics.)

Table 8 Summary of applications of various fiber optic sensing methods

Fiber Optic Sensor	Reference	Classification	Measurement parameters	Application object
Optical Fiber Grating Sensors	[97] [100] [101] [102] [103] [104] [105] [106] [107]	FBG	Temperature; Strain; RI; Flow Change	Battery/supercapacitor
		TFBG	SOC	
Optical Fiber Grating Sensors	[108] [109] [110] [111] [112] [113] [114] [115] [116] [117] [118] [119] [120] [121] [122]	MZI	Temperature; Strain	Battery
		FPI	Strain; SOC	
Optical Fiber Evanescent Wave Sensors	[123] [124] [125] [126]	OFEW	Electrolyte Density; SOC/SOH	Battery/supercapacitor
		SPR	SOC	
		LSPR	SOC	
Optical Fiber Photoluminescent Sensors	[80] [127]	Phosphorescence Intensity Measurement	Oxygen concentration	Battery
		Fluorescence Intensity Measurement	Temperature	
		Fluorescence Lifetime Measurement	Temperature	
Optical Fiber Scattering Sensors	[128] [129]	OFDR	Temperature; Strain	Battery

crucial. Currently, various sensing systems are flourishing in academia and industry, further improving the reliability of various new energy storage devices. However, several challenges remain in advancing the development of sensing systems.

1. The noise immunity of current and voltage sensors is a challenge as any disturbances can affect the quality of management, and almost all management strategies rely directly on such measurements. Although some advanced algorithms can be used to partially reduce the impact of disturbances on measurement quality, given the distributed nature of smart energy storage device management, the corresponding costs will be greatly increased.
2. Most of the important parts of the adopted methods are based on laboratory data, so there will be certain deviations and uncertainties in practical application. The measurement errors of these sensing systems and the resulting substantial errors in the algorithms can impact accuracy and robustness. In the future, it may be well to consider combining the adaptive forgetting recursive full least squares technique with a state observer (such as the Luenberger observer) to reduce the generated noise.
3. Embedded sensors can greatly simplify some data acquisition tasks, e.g., the temperature inside the battery can be directly measured, thus avoiding the tedious design of complex algorithms. However, this will lead to an increase in the cost of the entire system, so is an important factor in ensuring practicability and popularity.
4. Embedding sensors in practical new energy storage devices without affecting the performance is also a challenge. Optical fibers, for example, have demonstrated the advantages of high stability, corrosion resistance, and immunity to electromagnetic interference, but they are susceptible to severe bending or vibration in practical application, and this can seriously affect their performance. Therefore, effort is

needed to ensure the stability of fiber optic sensors as well as reasonable amplification and deployment.

5. There is a lack of connectivity between the fiber optic sensing system and the BMS algorithm and this results in inaccurate and time-consuming convergence rates. The interface and communication between the fiber optic sensor and the BMS could be improved by integrating electronic devices with the BMS hardware and appropriate networking technologies to accurately transfer the measurement information to the BMS.
6. Improving more dimensional information for next-generation BMS systems is also a challenge for sensing systems. In response to this problem, different optical fiber sensors could be integrated into one to achieve multi-channel measurement. At the same time, the distributed optical fiber sensing method could be adopted to achieve simultaneous high-sensitivity and high-precision measurement of multiple parameters in time and space.

Addressing these challenges will significantly contribute to the development of future sensing systems, and thus is crucial for the development and application of various novel energy storage devices.

4 Conclusion

In this paper, the measurement of key parameters such as current, voltage, temperature, and strain, all of which are closely related to the states of various new energy storage devices, and their relationship with the states of those devices are summarized and explained, mainly for non-embedded sensors and embedded sensors. Among them, non-embedded sensors diagnose their states by simply detecting a few characteristic signals such as external temperature, current, and voltage. They have the characteristics of simple operation and nondestructive measurement. However, it is not possible to sense the internal "black box" comprehensively to achieve early warning of safety accidents from the root. Integrated, miniature, embedded current/voltage sensors can measure parameters such as distribution currents and overpotentials that cannot be measured by external sensors, thus providing richer and more valuable information for managing the performance of new energy storage devices. Among them, fiber optic sensors have a greater advantage in both embedded and non-embedded measurements, especially for parameters such as temperature and strain. These parameters are not only used to track the dynamic chemistry of parasitic reactions but also of great relevance for use in predicting the SOC and SOH of batteries and supercapacitors as well as for end-of-life or predicting thermal runaway. Thus, composite sensors not relying excessively on complex algorithms while combined with fiber-optic sensors will be a research trend.

Abbreviations

SOC	State of charge
SOH	State of health
EV	Electric vehicle
HEV	Hybrid electric vehicle
RUL	Remaining useful life
QRL	Quality, reliability and life
ADC	Analog-to-digital converter
NXP	NXP semiconductors
FBG	Optical fiber Bragg grating
SPR	Surface plasmon resonance
MEMS	Microelectromechanical systems
MZI	Mach–Zehnder interferometer
OFEW	Optical fiber evanescent wave
FIM	Fluorescence intensity measurement
BMS	Battery management system
RTD	Resistance temperature detector
LIB	Lithium-ion battery
CNT	Carbon nanotube
EM	Electrochemical models
ECM	Equivalent circuit models
AIM	Artificial intelligence models
WDM	Wavelength division multiplexing
FPI	Fabry–Perot interferometer
RI	Refractive index
TFBG	Tilted fiber Bragg grating
SRI	Surrounding refractive index
LSPR	Localized surface plasmon resonance
OFDM	Organization of Fast Relief & Development
OFDR	Optical frequency domain reflectometry
PIM	Phosphorescence intensity measurement
FLM	Fluorescence lifetime measurement

Acknowledgements

This research was funded by the Youth Fund of Shandong Province Natural Science Foundation grant number ZR2020QE212, Key Projects of Shandong Province Natural Science Foundation grant number ZR2020KF020, the Guangdong Provincial Key Lab of Green Chemical Product Technology grant number GC 202111, Zhejiang Province Natural Science Foundation grant number LY22E070007 and National Natural Science Foundation of China grant number 52007170.

Author contributions

The named authors have substantially contributed to conducting the underlying research and drafting this manuscript. All authors read and approved the final manuscript.

Funding

This research was funded by the Youth Fund of Shandong Province Natural Science Foundation grant number ZR2020QE212, Key Projects of Shandong Province Natural Science Foundation grant number ZR2020KF020, the Guangdong Provincial Key Lab of Green Chemical Product Technology grant number GC 202111, Zhejiang Province Natural Science Foundation grant number LY22E070007 and National Natural Science Foundation of China grant number 52007170.

Availability of data and materials

The data and materials used to support the findings of this study are available from the corresponding author upon request.

Declarations

Competing interests
The authors declare that they have no known competing financial interests or personal relationships that could have appeared to influence the work reported in this paper.

Received: 4 January 2023 Accepted: 25 May 2023
Published online: 12 June 2023

References
1. Wei, Z. B., Hu, J., Li, Y., He, H. W., Li, W. H., & Sauer, D. U. (2022). Hierarchical soft measurement of load current and state of charge for future smart lithium-ion batteries. *Applied Energy, 307*, 118246. https://doi.org/10.1016/j.apenergy.2021.118246
2. Liu, C. L., Zhang, Y., Sun, J. R., Cui, Z. H., & Wang, K. (2022). Stacked bidirectional LSTM RNN to evaluate the remaining useful life of supercapacitor. *International Journal of Energy Research, 46*(3), 3034–3043. https://doi.org/10.1002/er.7360
3. Wang, L., Xie, L., Yang, Y., Zhang, Y., Wang, K., & Cheng, S. J. (2023). Distributed online voltage control with fast PV power fluctuations and imperfect communication. *IEEE Transactions on Smart Grid*. https://doi.org/10.1109/tsg.2023.3236724
4. Zhang, M., Yang, D., Du, J., Sun, H., Li, L., Wang, L., & Wang, K. (2023). A review of SOH prediction of Li-ion batteries based on data-driven algorithms. *Energies, 16*(7), 3167. https://doi.org/10.3390/en16073167
5. Zhang, M., Liu, Y., Li, D., Cui, X., Wang, L., Li, L., & Wang, K. (2023). Electrochemical impedance spectroscopy: A new chapter in the fast and accurate estimation of the state of health for lithium-ion batteries. *Energies, 16*(4), 1599. https://doi.org/10.3390/en16041599
6. Yu, X., Li, Y., Li, X., Wang, L., & Wang, K. (2023). Research on outdoor mobile music speaker battery management algorithm based on dynamic redundancy. *Technologies, 11*(2), 60. https://doi.org/10.3390/technologies11020060
7. Guo, Y., Yang, D., Zhang, Y., Wang, L., & Wang, K. (2022). Online estimation of SOH for lithium-ion battery based on SSA-Elman neural network. *Protection and Control of Modern Power Systems, 7*(1), 40. https://doi.org/10.1186/s41601-022-00261-y
8. Huang, J., Boles, S. T., & Tarascon, J.-M. (2022). Sensing as the key to battery lifetime and sustainability. *Nature Sustainability, 5*(3), 194–204. https://doi.org/10.1038/s41893-022-00859-y
9. Li, D., Wang, L., Duan, C., Li, Q., & Wang, K. (2022). Temperature prediction of lithium-ion batteries based on electrochemical impedance spectrum: A review. *International Journal of Energy Research, 46*(8), 10372–10388. https://doi.org/10.1002/er.7905
10. Cui, Z., Kang, L., Li, L., Wang, L., & Wang, K. (2022). A combined state-of-charge estimation method for lithium-ion battery using an improved BGRU network and UKF. *Energy, 259*, 124933. https://doi.org/10.1016/j.energy.2022.124933
11. Wang, R. L., Zhang, H. Z., Liu, Q. Y., Liu, F., Han, X. L., Liu, X. Q., Li, K. W., Xiao, G. Z., Albert, J., Lu, X. H., & Guo, T. (2022). Operando monitoring of ion activities in aqueous batteries with plasmonic fiber-optic sensors. *Nature Communications, 13*(1), 9452. https://doi.org/10.1038/s41467-022-28267-y
12. Han, G., Yan, J. Z., Guo, Z., Greenwood, D., Marco, J., & Yu, Y. F. (2021). A review on various optical fibre sensing methods for batteries. *Renewable & Sustainable Energy Reviews, 150*, 111514. https://doi.org/10.1016/j.rser.2021.111514
13. Li, D., Yang, D., Li, L., Wang, L., & Wang, K. (2022). Electrochemical impedance spectroscopy based on the state of health estimation for lithium-ion batteries. *Energies, 15*(18), 6665. https://doi.org/10.3390/en15186665
14. Su, Y. D., Preger, Y., Burroughs, H., Sun, C., & Ohodnicki, P. R. (2021). Fiber optic sensing technologies for battery management systems and energy storage applications. *Sensors, 21*(4), 1397. https://doi.org/10.3390/s21041397
15. Wahl, M. S., Spitthoff, L., Muri, H. I., Jinasena, A., Burheim, O. S., & Lamb, J. J. (2021). The importance of optical fibres for internal temperature sensing in lithium-ion batteries during operation. *Energies, 14*(12), 3617. https://doi.org/10.3390/en14123617
16. Wang, W., Yang, D., Huang, Z., Hu, H., Wang, L., & Wang, K. (2022). Electrodeless nanogenerator for dust recover. *Energy Technology, 10*(12), 2200699. https://doi.org/10.1002/ente.202200699
17. Peng, J., Jia, S. H., Yu, H. Q., Kang, X. L., Yang, S. M., & Xu, S. P. (2021). Design and experiment of FBG sensors for temperature monitoring on external electrode of lithium-ion batteries. *IEEE Sensors Journal, 21*(4), 4628–4634. https://doi.org/10.1109/jsen.2020.3034257
18. Wang, K., Li, L., Yin, H., Zhang, T., & Wan, W. (2015). Thermal modelling analysis of spiral wound supercapacitor under constant-current cycling. *PLoS ONE, 10*(10), e0138672. https://doi.org/10.1371/journal.pone.0138672
19. Yi, Z., Zhao, K., Sun, J., Wang, L., Wang, K., & Ma, Y. (2022). Prediction of the remaining useful life of supercapacitors. *Mathematical Problems in Engineering, 2022*, 7620382. https://doi.org/10.1155/2022/7620382
20. Cui, Z., Kang, L., Li, L., Wang, L., & Wang, K. (2022). A hybrid neural network model with improved input for state of charge estimation of lithium-ion battery at low temperatures. *Renewable Energy, 198*, 1328–1340. https://doi.org/10.1016/j.renene.2022.08.123
21. Wei, Z., Zhao, J., He, H., Ding, G., Cui, H., & Liu, L. (2021). Future smart battery and management: Advanced sensing from external to embedded multi-dimensional measurement. *Journal of Power Sources, 489*, 229462. https://doi.org/10.1016/j.jpowsour.2021.229462
22. Yu, Y. F., Vincent, T., Sansom, J., Greenwood, D., & Marco, J. (2022). Distributed internal thermal monitoring of lithium ion batteries with fibre sensors. *Journal of Energy Storage, 50*, 104291. https://doi.org/10.1016/j.est.2022.104291
23. Yang, L., Li, N., Hu, L., Wang, S., Wang, L., Zhou, J., Song, W.-L., Sun, L., Pan, T. S., Chen, H.-S., & Fang, D. (2021). Internal field study of 21700 battery based on long-life embedded wireless temperature sensor. *Acta Mechanica Sinica, 37*(6), 895–901. https://doi.org/10.1007/s10409-021-01103-0
24. Rente, B., Fabian, M., Vidakovic, M., Liu, X., Li, X., Li, K., Sun, T., & Grattan, K. T. V. (2021). Lithium-ion battery state-of-charge estimator based on FBG-based strain sensor and employing machine learning. *IEEE Sensors Journal, 21*(2), 1453–1460. https://doi.org/10.1109/jsen.2020.3016080
25. Zhang, M., Wang, K., & Zhou, Y. (2020). Online state of charge estimation of lithium-ion cells using particle filter-based hybrid filtering approach. *Complexity, 2020*, 8231243. https://doi.org/10.1155/2020/8231243
26. Liu, C., Li, D., Wang, L., Li, L., & Wang, K. (2022). Strong robustness and high accuracy in predicting remaining useful life of supercapacitors. *APL Materials, 10*(6), 061106. https://doi.org/10.1063/5.0092074
27. Wei, Z. B., Hu, J., He, H. W., Yu, Y. F., & Marco, J. (2023). Embedded distributed temperature sensing enabled multistate joint observation of smart lithium-ion battery. *IEEE Transactions on Industrial Electronics, 70*(1), 555–565. https://doi.org/10.1109/tie.2022.3146503
28. Angelopoulos, S., Misiaris, D., Banis, G., Liang, K., Tsarabaris, P., Ktena, A., & Hristoforou, E. (2020). Steel health monitoring device based on Hall sensors. *Journal of Magnetism and Magnetic Materials, 515*, 167304. https://doi.org/10.1016/j.jmmm.2020.167304
29. Atchison, H. L., Bailey, Z. R., Wetz, D. A., Davis, M., & Heinzel, J. M. (2021). Fiber optic based thermal and strain sensing of lithium-ion batteries at the individual cell level. *Journal of the Electrochemical Society, 168*(4), 040535. https://doi.org/10.1149/1945-7111/abf7e4
30. Zeng, Y., Chalise, D., Lubner, S. D., Kaur, S., & Prasher, R. S. (2021). A review of thermal physics and management inside lithium-ion batteries for high energy density and fast charging. *Energy Storage Materials, 41*, 264–288. https://doi.org/10.1016/j.ensm.2021.06.008
31. Parekh, M. H., Li, B., Palanisamy, M., Adams, T. E., Tomar, V., & Pol, V. G. (2020). In situ thermal runaway detection in lithium-ion batteries with an integrated internal sensor. *ACS Applied Energy Materials, 3*(8), 7997–8008. https://doi.org/10.1021/acsaem.0c01392
32. Zhang, M., Wang, W., Xia, G., Wang, L., & Wang, K. (2023). Self-powered electronic skin for remote human-machine synchronization. *ACS Applied Electronic Materials, 5*(1), 498–508. https://doi.org/10.1021/acsaelm.2c01476

33. Wang, W., Yang, D., Yan, X., Wang, L., Hu, H., & Wang, K. (2023). Triboelectric nanogenerators: The beginning of blue dream. *Frontiers of Chemical Science and Engineering*. https://doi.org/10.1007/s11705-022-2271-y
34. Stallard, J. C., Wheatcroft, L., Booth, S. G., Boston, R., Corr, S. A., De Volder, M. F. L., Inkson, B. J., & Fleck, N. A. (2022). Mechanical properties of cathode materials for lithium-ion batteries. *Joule, 6*(5), 984–1007. https://doi.org/10.1016/j.joule.2022.04.001
35. Yan, D. F., Dou, S., Tao, L., Liu, Z. J., Liu, Z. G., Huo, J., & Wang, S. Y. (2016). Electropolymerized supermolecule derived N, P co-doped carbon nanofiber networks as a highly efficient metal-free electrocatalyst for the hydrogen evolution reaction. *Journal of Materials Chemistry A, 4*(36), 13726–13730. https://doi.org/10.1039/c6ta05863a
36. Zhu, S. X., Han, J. D., An, H. Y., Pan, T. S., Wei, Y. M., Song, W. L., Chen, H. S., & Fang, D. N. (2020). A novel embedded method for in-situ measuring internal multi-point temperatures of lithium ion batteries. *Journal of Power Sources, 456*, 227981. https://doi.org/10.1016/j.jpowsour.2020.227981
37. Ghannoum, A., Nieva, P., Yu, A. P., & Khajepour, A. (2017). Development of embedded fiber-optic evanescent wave sensors for optical characterization of graphite anodes in lithium-ion batteries. *ACS Applied Materials & Interfaces, 9*(47), 41284–41290. https://doi.org/10.1021/acsami.7b13464
38. Hedman, J., & Bjorefors, F. (2022). Fiber optic monitoring of composite lithium iron phosphate cathodes in pouch cell batteries. *ACS Applied Energy Materials, 5*(1), 870–881. https://doi.org/10.1021/acsaem.1c03304
39. Fleming, J., Amietszajew, T., McTurk, E., Towers, D. P., Greenwood, D., & Bhagat, R. (2018). Development and evaluation of in-situ instrumentation for cylindrical Li-ion cells using fibre optic sensors. *HardwareX, 3*, 100–109. https://doi.org/10.1016/j.ohx.2018.04.001
40. Nascimento, M., Ferreira, M. S., & Pinto, J. L. (2017). Real time thermal monitoring of lithium batteries with fiber sensors and thermocouples: A comparative study. *Measurement, 111*, 260–263. https://doi.org/10.1016/j.measurement.2017.07.049
41. Waldmann, T., Bisle, G., Hogg, B. I., Stumpp, S., Danzer, M. A., Kasper, M., Axmann, P., & Wohlfahrt-Mehrens, M. (2015). Influence of cell design on temperatures and temperature gradients in lithium-ion cells: An in operando study. *Journal of the Electrochemical Society, 162*(6), A921–A927. https://doi.org/10.1149/2.0561506jes
42. Tippmann, S., Walper, D., Balboa, L., Spier, B., & Bessler, W. G. (2014). Low-temperature charging of lithium-ion cells part I: Electrochemical modeling and experimental investigation of degradation behavior. *Journal of Power Sources, 252*, 305–316. https://doi.org/10.1016/j.jpowsour.2013.12.022
43. Che Daud, Z. H., Chrenko, D., Dos Santos, F., Aglzim, E.-H., Keromnes, A., & Le Moyne, L. (2016). 3D electro-thermal modelling and experimental validation of lithium polymer-based batteries for automotive applications. *International Journal of Energy Research, 40*(8), 1144–1154. https://doi.org/10.1002/er.3524
44. Chalise, D., Shah, K., Halama, T., Komsiyska, L., & Jain, A. (2017). An experimentally validated method for temperature prediction during cyclic operation of a Li-ion cell. *International Journal of Heat and Mass Transfer, 112*, 89–96. https://doi.org/10.1016/j.ijheatmasstransfer.2017.04.115
45. Hegde, G., Himakar, B., Rao, M. V. S., Hegde, G., & Asokan, S. (2022). Simultaneous measurement of pressure and temperature in a supersonic ejector using FBG sensors. *Measurement Science and Technology, 33*(12), 125111. https://doi.org/10.1088/1361-6501/ac8a0a
46. Louli, A. J., Ellis, L. D., & Dahn, J. R. (2019). Operando pressure measurements reveal solid electrolyte interphase growth to rank Li-ion cell performance. *Joule, 3*(3), 745–761. https://doi.org/10.1016/j.joule.2018.12.009
47. Liang, Q., Zhang, D., Coppola, G., Wang, Y., Wei, S., & Ge, Y. (2014). Multidimensional MEMS/micro sensor for force and moment sensing: A review. *IEEE Sensors Journal, 14*(8), 2643–2657. https://doi.org/10.1109/jsen.2014.2313860
48. Nascimento, M., Ferreira, M. S., & Pinto, J. L. (2019). Temperature fiber sensing of Li-ion batteries under different environmental and operating conditions. *Applied Thermal Engineering, 149*, 1236–1243. https://doi.org/10.1016/j.applthermaleng.2018.12.135
49. Arslan, M. M., & Bayrak, G. (2022). Temperature compensation of FBG sensors via sensor packaging approach for harsh environmental applications. *Gazi University Journal of Science, 35*(4), 1471–1482. https://doi.org/10.35378/gujs.981290
50. Lee, J. H., Lee, H. M., & Ahn, S. (2003). Battery dimensional changes occurring during charge/discharge cycles—thin rectangular lithium ion and polymer cells. *Journal of Power Sources, 119–121*, 833–837. https://doi.org/10.1016/S0378-7753(03)00281-7
51. Oh, K.-Y., Siegel, J. B., Secondo, L., Kim, S. U., Samad, N. A., Qin, J., Anderson, D., Garikipati, K., Knobloch, A., Epureanu, B. I., Monroe, C. W., & Stefanopoulou, A. (2014). Rate dependence of swelling in lithium-ion cells. *Journal of Power Sources, 267*, 197–202. https://doi.org/10.1016/j.jpowsour.2014.05.039
52. Dai, H., Yu, C., Wei, X., & Sun, Z. (2017). State of charge estimation for lithium-ion pouch batteries based on stress measurement. *Energy, 129*, 16–27. https://doi.org/10.1016/j.energy.2017.04.099
53. Guo, Y., Yu, P., Zhu, C., Zhao, K., Wang, L. C., & Wang, K. (2022). A state-of-health estimation method considering capacity recovery of lithium batteries. *International Journal of Energy Research, 46*(15), 23730–23745. https://doi.org/10.1002/er.8671
54. Wang, X. M., Sone, Y., Segami, G., Naito, H., Yamada, C., & Kibe, K. (2007). Understanding volume change in lithium-ion cells during charging and discharging using in situ measurements. *Journal of the Electrochemical Society, 154*(1), A14–A21. https://doi.org/10.1149/1.2386933
55. Cannarella, J., & Arnold, C. B. (2014). Stress evolution and capacity fade in constrained lithium-ion pouch cells. *Journal of Power Sources, 245*, 745–751. https://doi.org/10.1016/j.jpowsour.2013.06.165
56. Knobloch, A., Kapusta, C., Karp, J., Plotnikov, Y., Siegel, J. B., & Stefanopoulou, A. G. (2018). Fabrication of multimeasurand sensor for monitoring of a Li-ton battery. *Journal of Electronic Packaging, 140*(3), 031002. https://doi.org/10.1115/1.4039861
57. Choi, W., Seo, Y., Yoo, K., Ko, T.J. & Choi, J. (2019). Carbon nanotube-based strain sensor for excessive swelling detection of lithium-ion battery. in *2019 20th International conference on solid-state sensors, actuators and microsystems & Eurosensors XXXIII, IEEE, 2019*, 2356–2359. https://doi.org/10.1109/TRANSDUCERS.2019.8808477
58. Peng, J., Zhou, X., Jia, S. H., Jin, Y. M., Xu, S. P., & Chen, J. Z. (2019). High precision strain monitoring for lithium ion batteries based on fiber Bragg grating sensors. *Journal of Power Sources, 433*, 226692. https://doi.org/10.1016/j.jpowsour.2019.226692
59. Peng, J., Jia, S. H., Jin, Y. M., Xu, S. P., & Xu, Z. D. (2019). Design and investigation of a sensitivity-enhanced fiber Bragg grating sensor for microstrain measurement. *Sensors and Actuators a-Physical, 285*, 437–447. https://doi.org/10.1016/j.sna.2018.11.038
60. Sommer, L. W., Raghavan, A., KieseL, P., Saha, B., Schwartz, J., Lochbaum, A., Ganguli, A., Bae, C.-J., & Alamgir, M. (2015). Monitoring of intercalation stages in lithium-ion cells over charge-discharge cycles with fiber optic sensors. *Journal of the Electrochemical Society, 162*(14), A2664–A2669. https://doi.org/10.1149/2.0361514jes
61. Nascimento, M., Ferreira, M. S., & Pinto, J. L. (2018). Simultaneous Sensing of temperature and Bi-directional strain in a prismatic Li-ion battery. *Batteries-Basel, 4*(2), 23. https://doi.org/10.3390/batteries4020023
62. Raijmakers, L. H. J., Danilov, D. L., Eichel, R. A., & Notten, P. H. L. (2019). A review on various temperature-indication methods for Li-ion batteries. *Applied Energy, 240*, 918–945. https://doi.org/10.1016/j.apenergy.2019.02.078
63. Lim, S., & Suk, J. W. (2023). Flexible temperature sensors based on two-dimensional materials for wearable devices. *Journal of Physics D-Applied Physics, 56*(6), 063001. https://doi.org/10.1088/1361-6463/acaf38
64. Xue, Q., Li, G., Zhang, Y., Shen, S., Chen, Z., & Liu, Y. (2021). Fault diagnosis and abnormality detection of lithium-ion battery packs based on statistical distribution. *Journal of Power Sources, 482*(15), 228964. https://doi.org/10.1016/j.jpowsour.2020.228964
65. Hossain Lipu, M. S., Hannan, M. A., Karim, T. F., Hussain, A., Saad, M. H. M., Ayob, A., Miah, M. S., & Indra Mahlia, T. M. (2021). Intelligent algorithms and control strategies for battery management system in electric vehicles: Progress, challenges and future outlook. *Journal of Cleaner Production, 292*, 126044. https://doi.org/10.1016/j.jclepro.2021.126044
66. Xia, Q., Li, X., Wang, K., Li, Z., Liu, H., Wang, X., Ye, W., Li, H., Teng, X., Pang, J., Zhang, Q., Ge, C., Gu, L., Miao, G. X., Yan, S., Hu, H., & Li, Q. (2022). Unraveling the evolution of transition metals during Li alloying-dealloying by in-operando magnetometry. *Chemistry of Materials, 34*(13), 5852–5859. https://doi.org/10.1021/acs.chemmater.2c00618

67. Cambron, D. C., & Cramer, A. M. (2017). A lithium-ion battery current estimation technique using an unknown input observer. *IEEE Transactions on Vehicular Technology, 66*(8), 6707–6714. https://doi.org/10.1109/tvt.2017.2657520
68. Wang, C., Wang, S. L., Zhou, J. Z., & Qiao, J. L. (2022). A novel BCRLS-BP-EKF method for the state of charge estimation of lithium-ion batteries. *International Journal of Electrochemical Science, 17*(4), 220431. https://doi.org/10.20964/2022.04.53
69. Jiang, C., Wang, S. L., Wu, B., Fernandez, C., Xiong, X., & Coffie-Ken, J. (2021). A state-of-charge estimation method of the power lithium-ion battery in complex conditions based on adaptive square root extended Kalman filter. *Energy, 219*, 119603. https://doi.org/10.1016/j.energy.2020.119603
70. Poopanya, P., Sivalertporn, K., & Phophongviwat, T. (2022). A comparative study on the parameter identification of an equivalent circuit model for an Li-Ion battery based on different discharge tests. *World Electric Vehicle Journal, 13*(3), 50. https://doi.org/10.3390/wevj13030050
71. Dao, V., Dinh, M. C., Kim, C. S., Park, M., Doh, C. H., Bae, J. H., Lee, M. K., Liu, J., & Bai, Z. (2021). Design of an effective state of charge estimation method for a lithium-ion battery pack using extended Kalman filter and artificial neural network. *Energies, 14*(9), 2634. https://doi.org/10.3390/en14092634
72. Chen, N., Zhao, X., Chen, J. Y., Xu, X. D., Zhang, P., & Gui, W. H. (2022). Design of a non-linear observer for SOC of lithium-ion battery based on neural network. *Energies, 15*(10), 3835. https://doi.org/10.3390/en15103835
73. Lee, C.-Y., Peng, H.-C., Lee, S.-J., Hung, I. M., Hsieh, C.-T., Chiou, C.-S., Chang, Y.-M., & Huang, Y.-P. (2015). A flexible three-in-one microsensor for real-time monitoring of internal temperature, voltage and current of lithium batteries. *Sensors, 15*(5), 11485–11498. https://doi.org/10.3390/s150511485
74. Fleming, J., Amietszajew, T., Charmet, J., Roberts, A. J., Greenwood, D., & Bhagat, R. (2019). The design and impact of in-situ and operando thermal sensing for smart energy storage. *Journal of Energy Storage, 22*, 36–43. https://doi.org/10.1016/j.est.2019.01.026
75. Li, Z., Zhang, J. B., Wu, B., Huang, J., Nie, Z. H., Sun, Y., An, F. Q., & Wu, N. N. (2013). Examining temporal and spatial variations of internal temperature in large-format laminated battery with embedded thermocouples. *Journal of Power Sources, 241*, 536–553. https://doi.org/10.1016/j.jpowsour.2013.04.117
76. Waldmann, T., & Wohlfahrt-Mehrens, M. (2015). In-operando measurement of temperature gradients in cylindrical lithium-ion cells during high-current discharge. *ECS Electrochemistry Letters, 4*(1), A1–A3. https://doi.org/10.1149/2.0031501eel
77. Anthony, D., Wong, D., Wetz, D., & Jain, A. (2017). Non-invasive measurement of internal temperature of a cylindrical Li-ion cell during high-rate discharge. *International Journal of Heat and Mass Transfer, 111*, 223–231. https://doi.org/10.1016/j.ijheatmasstransfer.2017.03.095
78. Raghavan, A., Kiesel, P., Sommer, L. W., Schwartz, J., Lochbaum, A., Hegyi, A., Schuh, A., Arakaki, K., Saha, B., Ganguli, A., Kim, K. H., Kim, C., Hah, H. J., Kim, S., Hwang, G.-O., Chung, G.-C., Choi, B., & Alamgir, M. (2017). Embedded fiber-optic sensing for accurate internal monitoring of cell state in advanced battery management systems part 1: Cell embedding method and performance. *Journal of Power Sources, 341*, 466–473. https://doi.org/10.1016/j.jpowsour.2016.11.104
79. Bae, C. J., Manandhar, A., Kiesel, P., & Raghavan, A. (2016). Monitoring the strain evolution of lithium-ion battery electrodes using an optical fiber Bragg grating sensor. *Energy Technology, 4*(7), 851–855. https://doi.org/10.1002/ente.201500514
80. Novais, S., Nascimento, M., Grande, L., Domingues, M. F., Antunes, P., Alberto, N., Leitão, C., Oliveira, R., Koch, S., Kim, G. T., Passerini, S., & Pinto, J. (2016). Internal and external temperature monitoring of a Li-Ion battery with fiber Bragg grating sensors. *Sensors (Basel, Switzerland), 16*(9), 1394. https://doi.org/10.3390/s16091394
81. McTurk, E., Amietszajew, T., Fleming, J., & Bhagat, R. (2018). Thermo-electrochemical instrumentation of cylindrical Li-ion cells. *Journal of Power Sources, 379*, 309–316. https://doi.org/10.1016/j.jpowsour.2018.01.060
82. Amietszajew, T., McTurk, E., Fleming, J., & Bhagat, R. (2018). Understanding the limits of rapid charging using instrumented commercial 18650 high-energy Li-ion cells. *Electrochimica Acta, 263*, 346–352. https://doi.org/10.1016/j.electacta.2018.01.076
83. Lee, C. Y., Lee, S. J., Hung, Y. M., Hsieh, C. T., Chang, Y. M., Huang, Y. T., & Lin, J. T. (2017). Integrated microsensor for real-time microscopic monitoring of local temperature, voltage and current inside lithium ion battery. *Sensors and Actuators a-Physical, 253*, 59–68. https://doi.org/10.1016/j.sna.2016.10.011
84. Zhou, W. H., Ye, Q., Ye, L., Li, X., Zeng, C. Z., Huang, C., Cai, H. W., & Qu, R. H. (2020). Distributed optical fiber in-situ monitoring technology for a healthy temperature field in lithium ion batteries. *Chinese Journal of Lasers-Zhongguo Jiguang, 47*(12), 1204002. https://doi.org/10.3788/cjl202047.1204002
85. Nedjalkov, A., Meyer, J., Graefenstein, A., Schramm, B., Angelmahr, M., Schwenzel, J., & Schade, W. (2019). Refractive index measurement of lithium ion battery electrolyte with etched surface cladding waveguide Bragg gratings and cell electrode state monitoring by optical strain sensors. *Batteries-Basel, 5*(1), 5010030. https://doi.org/10.3390/batteries5010030
86. Cheng, X. M., & Pecht, M. (2017). In situ stress measurement techniques on Li-ion battery electrodes: A review. *Energies, 10*(5), 10050591. https://doi.org/10.3390/en10050591
87. Sun, H., Yang, D., Wang, L., & Wang, K. (2022). A method for estimating the aging state of lithium-ion batteries based on a multi-linear integrated model. *International Journal of Energy Research, 46*(15), 24091–24104. https://doi.org/10.1002/er.8709
88. Fortier, A., Tsao, M., Williard, N., Xing, Y., & Pecht, M. (2017). Preliminary study on integration of fiber optic Bragg grating sensors in Li-Ion batteries and in situ strain and temperature monitoring of battery cells. *Energies, 10*(7), 838. https://doi.org/10.3390/en10070838
89. Huang, J., Albero Blanquer, L., Bonefacino, J., Logan, E., Alves Dalla Corte, D., Delacourt, C., Gallant, B., Boles, S., Dahn, J., Tam, H., & Tarascon, J. M. (2020). Operando decoding of chemical and thermal events in commercial Na(Li)-ion cells via optical sensors. *Nature Energy, 5*, 1–10. https://doi.org/10.1038/s41560-020-0665-y
90. Nedjalkov, A., Meyer, J., Grafenstein, A., Schramm, B., Angelmahr, M., Schwenzel, J., & Schade, W. (2019). Refractive Index Measurement of Lithium Ion Battery Electrolyte with Etched Surface Cladding Waveguide Bragg Gratings and Cell Electrode State Monitoring by Optical Strain Sensors. *Batteries-Basel, 5*(1), 5010030. https://doi.org/10.3390/batteries5010030
91. Huang, J. Q., Blanquer, L. A., Bonefacino, J., Logan, E. R., Dalla Corte, D. A., Delacourt, C., Gallant, B. M., Boles, S. T., Dahn, J. R., Tam, H. Y., & Tarascon, J. M. (2020). Operando decoding of chemical and thermal events in commercial Na(Li)-ion cells via optical sensors. *Nature Energy, 5*(9), 674–683. https://doi.org/10.1038/s41560-020-0665-y
92. Nascimento, M., Novais, S., Ding, M. S., Ferreira, M. S., Koch, S., Passerini, S., & Pinto, J. L. (2019). Internal strain and temperature discrimination with optical fiber hybrid sensors in Li-ion batteries. *Journal of Power Sources, 410*, 1–9. https://doi.org/10.1016/j.jpowsour.2018.10.096
93. Liu, X., Liang, L., Jiang, K., & Xu, G. (2020). Sensitivity-enhanced fiber Bragg grating pressure sensor based on a diaphragm and hinge-lever structure. *IEEE Sensors Journal, 21*(7), 9155–9164. https://doi.org/10.1109/JSEN.2020.3045992
94. Zhu, B. Y., Zheng, T. L., Xiong, J. W., Shi, X. T., Cheng, Y. J., & Xia, Y. G. (2022). A lithium-ion battery cathode with enhanced wettability toward an electrolyte fabricated by a fast light curing of photoactive slurry. *Energy & Fuels, 36*(6), 3313–3318. https://doi.org/10.1021/acs.energyfuels.1c04441
95. Wang, Y., Tian, J., Sun, Z., Wang, L., Xu, R., Li, M., & Chen, Z. (2020). A comprehensive review of battery modeling and state estimation approaches for advanced battery management systems. *Renewable and Sustainable Energy Reviews, 131*, 110015. https://doi.org/10.1016/j.rser.2020.110015
96. Sun, H., Sun, J., Zhao, K., Wang, L., & Wang, K. (2022). Data-driven ICA-Bi-LSTM-combined lithium battery SOH estimation. *Mathematical Problems in Engineering*, *2022*, 1–8. https://doi.org/10.1155/2022/9645892
97. Lao, J., Sun, P., Liu, F., Zhang, X., Zhao, C., Mai, W., Guo, T., Xiao, G., & Albert, J. (2018). In situ plasmonic optical fiber detection of the state of charge of supercapacitors for renewable energy storage. *Light: Science & Applications, 7*(1), 34. https://doi.org/10.1038/s41377-018-0040-y
98. Ghannoum, A., Norris, R. C., Iyer, K., Zdravkova, L., Yu, A., & Nieva, P. (2016). Optical characterization of commercial lithiated graphite battery electrodes and in situ fiber optic evanescent wave spectroscopy. *ACS*

Applied Materials & Interfaces, 8(29), 18763–18769. https://doi.org/10.1021/acsami.6b03638
99. Qian, S., Chen, X., Jiang, S., Pan, Q., Gao, Y., Wang, L., Peng, W., Liang, S., Zhu, J., & Liu, S. (2020). Direct detection of charge and discharge process in supercapacitor by fiber-optic LSPR sensors. *Nanophotonics, 9*(5), 1071–1079. https://doi.org/10.1515/nanoph-2019-0504
100. Dhanalakshmi, S., Nandini, P., Rakshit, S., Rawat, P., Narayanamoorthi, R., Kumar, R., & Senthil, R. (2022). Fiber Bragg grating sensor-based temperature monitoring of solar photovoltaic panels using machine learning algorithms. *Optical Fiber Technology, 69*, 102831. https://doi.org/10.1016/j.yofte.2022.102831
101. Wu, H., Huang, C., Cui, R., & Zhou, J. (2022). Simulation and experiment analysis of temperature field of magnetic suspension support based on FBG. *Sensors (Basel), 22*(12), 4350. https://doi.org/10.3390/s22124350
102. David, N. A., Wild, P. M., Jensen, J., Navessin, T., & Djilali, N. (2010). Simultaneous in situ measurement of temperature and relative humidity in a PEMFC using optical fiber sensors. *Journal of The Electrochemical Society, 157*(8), B1173. https://doi.org/10.1149/1.3436652
103. Yang, G., Leitão, C., Li, Y., Pinto, J., & Jiang, X. (2013). Real-time temperature measurement with fiber Bragg sensors in lithium batteries for safety usage. *Measurement, 46*(9), 3166–3172. https://doi.org/10.1016/j.measurement.2013.05.027
104. Sommer, L. W., Kiesel, P., Ganguli, A., Lochbaum, A., Saha, B., Schwartz, J., Bae, C.-J., Alamgir, M., & Raghavan, A. (2015). Fast and slow ion diffusion processes in lithium ion pouch cells during cycling observed with fiber optic strain sensors. *Journal of Power Sources, 296*, 46–52. https://doi.org/10.1016/j.jpowsour.2015.07.025
105. Osuch, T., Jurek, T., Markowski, K., & Jedrzejewski, K. (2016). Simultaneous measurement of liquid level and temperature using tilted fiber Bragg grating. *IEEE Sensors Journal, 16*(5), 1205–1209. https://doi.org/10.1109/JSEN.2015.2501381
106. Li, Y., Li, K., Liu, X., Li, X., Zhang, L., Rente, B., Sun, T., & Grattan, K. T. V. (2022). A hybrid machine learning framework for joint SOC and SOH estimation of lithium-ion batteries assisted with fiber sensor measurements. *Applied Energy, 325*, 119787. https://doi.org/10.1016/j.apenergy.2022.119787
107. Wu, Y., Long, X., Lu, J., Zhou, R., Liu, L., & Wu, Y. (2023). Long-life in-situ temperature field monitoring using fiber Bragg grating sensors in electromagnetic launch high-rate hardcase lithium-ion battery. *Journal of Energy Storage, 57*, 106207. https://doi.org/10.1016/j.est.2022.106207
108. Sun, X., Du, H., Dong, X., Hu, Y., & Duan, J. A. (2020). Simultaneous curvature and temperature sensing based on a novel Mach–Zehnder interferometer. *Photonic Sensors, 10*(2), 171–180. https://doi.org/10.1007/s13320-019-0551-z
109. Peng, J., Jia, S., Yang, S., Kang, X., Yu, H., & Yang, Y. (2022). State estimation of lithium-ion batteries based on strain parameter monitored by fiber Bragg grating sensors. *Journal of Energy Storage, 52*, 104950. https://doi.org/10.1016/j.est.2022.104950
110. Zhao, Y., Xia, F., & Chen, M. (2017). Curvature sensor based on Mach–Zehnder interferometer with vase-shaped tapers. *Sensors and Actuators A: Physical, 265*, 275–279. https://doi.org/10.1016/j.sna.2017.09.005
111. Wu, J., Yin, M., Seefeldt, K., Dani, A., Guterman, R., Yuan, J., Zhang, A. P., & Tam, H. (2018). In situ μ-printed optical fiber-tip CO_2 sensor using a photocrosslinkable poly(ionic liquid). *Sensors and Actuators B: Chemical, 259*, 833–839. https://doi.org/10.1016/j.snb.2017.12.125
112. Li, Y., Wang, W., Yang, X.-G., Zuo, F., Liu, S., & Lin, C. (2022). A smart Li-ion battery with self-sensing capabilities for enhanced life and safety. *Journal of Power Sources, 546*, 231705. https://doi.org/10.1016/j.jpowsour.2022.231705
113. Liu, Z., Gu, X., Wu, C., Ren, H., Zhou, Z., & Tang, S. (2022). Studies on the validity of strain sensors for pavement monitoring: A case study for a fiber Bragg grating sensor and resistive sensor. *Construction and Building Materials, 321*, 126085. https://doi.org/10.1016/j.conbuildmat.2021.126085
114. Xu, X., Wang, Y., Zhu, D., & Shi, J. (2022). Accurate strain extraction via kernel extreme learning machine for fiber Bragg grating sensor. *IEEE Sensors Journal, 22*(8), 7792–7797. https://doi.org/10.1109/JSEN.2022.3156595
115. Pan, Y., Liu, T., Jiang, J., Liu, K., Wang, S., Yin, J., He, P., & Yan, J. (2015). Simultaneous measurement of temperature and strain using spheroidal-cavity-overlapped FBG. *IEEE Photonics Journal, 7*(6), 1–6. https://doi.org/10.1109/JPHOT.2015.2493724
116. Liu, Y., Zhang, T., Wang, Y., Yang, D., Liu, X., Fu, H., & Jia, Z. (2018). Simultaneous measurement of gas pressure and temperature with integrated optical fiber FPI sensor based on in-fiber micro-cavity and fiber-tip. *Optical Fiber Technology, 46*, 77–82. https://doi.org/10.1016/j.yofte.2018.09.021
117. Liu, Y., Yang, D., Wang, Y., Zhang, T., Shao, M., Yu, D., Fu, H., & Jia, Z. (2019). Fabrication of dual-parameter fiber-optic sensor by cascading FBG with FPI for simultaneous measurement of temperature and gas pressure. *Optics Communications, 443*, 166–171. https://doi.org/10.1016/j.optcom.2019.03.034
118. Li, Q., Wang, J., Mu, H., Lv, J., Yang, L., Shi, Y., Yi, Z., Chu, P. K., Liu, Q., & Liu, C. (2023). A Fabry–Pérot interferometer strain sensor composed of a rounded rectangular air cavity with a thin wall for high sensitivity and interference contrast. *Optics Communications, 527*, 128920. https://doi.org/10.1016/j.optcom.2022.128920
119. Hou, D., Kang, J., Wang, L., Zhang, Q., Zhao, Y., & Zhao, C. (2019). Bare fiber adapter based Fabry–Pérot interferometer for microfluidic velocity measurement. *Optical Fiber Technology, 50*, 71–75. https://doi.org/10.1016/j.yofte.2019.02.013
120. Moslan, M. S., Othman, M. H. D., Samavati, A., Theodosiou, A., Kalli, K., Ismail, A. F., & Rahman, M. A. (2023). Real-time fluid flow movement identification in porous media for reservoir monitoring application using polycarbonate optical fibre Bragg grating sensor. *Sensors and Actuators A: Physical, 354*(1), 114246. https://doi.org/10.1016/j.sna.2023.114246
121. Fan, H., Zhang, L., Gao, S., Chen, L., & Bao, X. (2019). Ultrasound sensing based on an in-fiber dual-cavity Fabry–Perot interferometer. *Optics Letters, 44*(15), 3606–3609. https://doi.org/10.1364/OL.44.003606
122. Costa, G. K. B., Gouvêa, P. M. P., Soares, L. M. B., Pereira, J. M. B., Favero, F., Braga, A. M. B., Palffy-Muhoray, P., Bruno, A. C., & Carvalho, I. C. S. (2016). In-fiber Fabry–Perot interferometer for strain and magnetic field sensing. *Optics Express, 24*(13), 14690–14696. https://doi.org/10.1364/OE.24.014690
123. Yin, M.-J., Gu, B., An, Q.-F., Yang, C., Guan, Y. L., & Yong, K.-T. (2018). Recent development of fiber-optic chemical sensors and biosensors: Mechanisms, materials, micro/nano-fabrications and applications. *Coordination Chemistry Reviews, 376*, 348–392. https://doi.org/10.1016/j.ccr.2018.08.001
124. Liang, G., Luo, Z., Liu, K., Wang, Y., Dai, J., & Duan, Y. (2016). Fiber optic surface plasmon resonance-based biosensor technique: Fabrication, advancement, and application. *Critical Reviews in Analytical Chemistry, 46*(3), 213–223. https://doi.org/10.1080/10408347.2015.1045119
125. Zhong, J. L., Liu, S., Zou, T., Yan, W. Q., Zhou, M., Liu, B. A., Rao, X., Wang, Y., Sun, Z. Y., & Wang, Y. P. (2022). All fiber-optic immunosensors based on elliptical core helical intermediate-period fiber grating with low-sensitivity to environmental disturbances. *Biosensors-Basel, 12*(2), 99. https://doi.org/10.3390/bios12020099
126. Hasler, R., Reiner-Rozman, C., Fossati, S., Aspermair, P., Dostalek, J., Lee, S., Ibanez, M., Bintinger, J., & Knoll, W. (2022). Field-effect transistor with a plasmonic fiber optic gate electrode as a multivariable biosensor device. *ACS Sensors, 7*(2), 504–512. https://doi.org/10.1021/acssensors.1c02313
127. Fujimoto, S., Uemura, S., Imanishi, N., & Hirai, S. (2019). Oxygen concentration measurement in the porous cathode of a lithium-air battery using a fine optical fiber sensor. *Mechanical Engineering Letters, 5*, 19–00095. https://doi.org/10.1299/mel.19-00095
128. Yu, Y., Vergori, E., Worwood, D., Tripathy, Y., Guo, Y., Somá, A., Greenwood, D., & Marco, J. (2021). Distributed thermal monitoring of lithium ion batteries with optical fibre sensors. *Journal of Energy Storage, 39*, 102560. https://doi.org/10.1016/j.est.2021.102560
129. Vergori, E., & Yu, Y. (2019). Monitoring of Li-ion cells with distributed fibre optic sensors. *Procedia Structural Integrity, 24*, 233–239. https://doi.org/10.1016/j.prostr.2020.02.020
130. Yu, X. F., Ma, N., Zheng, L., Wang, L. C., & Wang, K. (2023). Developments and applications of artificial intelligence in music education. *Technologies, 11*(2), 42. https://doi.org/10.3390/technologies11020042
131. Ma, N., Yang, D. F., Riaz, S., Wang, L. C., & Wang, K. (2023). Aging mechanism and models of supercapacitors: A review. *Technologies, 11*(2), 38. https://doi.org/10.3390/technologies11020038\